IN-22094

NASA Contractor Report 172461

Batten Augmented Triangular Beam

Louis R. Adams and John M. Hedgepeth
Astro Aerospace Corporation
Carpinteria, California

Prepared for
Langley Research Center
under Contract NAS1-17536
February 1986

National Aeronautics and
Space Administration
Langley Research Center
Hampton, Virginia 23665

NASA Contractor Report 172461

Batten Augmented Triangular Beam

Louis R. Adams and John M. Hedgepeth
Astro Aerospace Corporation
Carpinteria, California

Prepared for
Langley Research Center
under Contract NAS1-16134

February 1986

National Aeronautics and
Space Administration

Langley Research Center
Hampton, Virginia 23665

TABLE OF CONTENTS

LIST OF TABLES AND FIGURES

SECTION 1
INTRODUCTION

All of the structures constructed in space have been automatically deployed by inflation (Echo), strain release (Astromast), or by relatively simple mechanisms (STEMs, TEEs, scissors devices, etc.). In order to establish larger and more efficient structures in space, different techniques are required. For example, many future structures will be composed of large trusses that must be formed in space either by deployment with complex mechanisms, assembly by man and/or machine, fabrication by machine, or some combination of these. In order to make these advanced techniques available to future missions, research is needed on generic approaches for space construction.

Under contract to NASA, Astro Aerospace Corporation (Astro) is helping to develop the technology base for large structures. This paper is one of a number that are being used to report on the various tasks associated with the research. This particular note deals with the structural behavior during and after deployment of a NASA LaRC-generated concept termed the "BAT Beam." Also included is the conceptual design of a suitable deployer for the BAT Beam.

In numerous places in this paper, examples are given to clarify the results of analyses. These examples are for a specific BAT Beam which is described in Table 1.

SECTION 2
BAT BEAM STRUCTURAL ANALYSIS

The BAT (Batten-Augmented Triangular) Beam is shown in Figure 1. The lengths and properties of the various members cause preloads in the deployed structure so that the diagonals are in tension, the battens are buckled in compression, and the longerons are in compression at less than their buckling load. These lengths and properties are presented in Table 1.

The nominal behavior of the deployed BAT Beam is analyzed in the remainder of this section.

2.1 PRELOAD DISTRIBUTION

The preload distribution in the BAT Beam is determined as follows. At a generic Point A in the beam (see Figure 1), the buckled battens exert a force P_B independent of the degree of bowing of the battens. The tensioned diagonals have tension T_{d_n} to the left and $T_{d_{n+1}}$ to the right. Longeron compressions are P_{ℓ_n} to the left and $P_{\ell_{n+1}}$ to the right. Note that, throughout this paper, the convention is used in which the positive values of P denote compression in the longerons and battens and positive values of T denote tension in the diagonals.

The sum of the loads in the x direction is

$$\sum F_x = \left(2T_{d_n} + 2T_{d_{n+1}}\right) \cos\beta \cos 30^\circ - 2P_B \cos 30^\circ = 0$$

or

$$T_{d_n} + T_{d_{n+1}} = \frac{P_B}{\cos\beta} \qquad (1)$$

The sum of the loads in the z direction is

$$\sum F_z = -2T_{d_n} \sin\beta + P_{\ell_n} + 2T_{d_{n+1}} \sin\beta - P_{\ell_{n+1}} = 0$$

or

$$P_{\ell_n} - 2T_{d_n} \sin \beta = P_{\ell_{n+1}} - 2T_{d_{n+1}} \sin \beta \qquad (2)$$

Equations (1) and (2) are solvable by recursion starting at either end of the beam. Consider the left end for which n = 0. For zero external loading, P_0 and T_0 are zero. Thus,

$$T_{d_1} = \frac{P_{B\ end}}{\cos \beta}$$

and

$$P_{\ell_1} = 2T_{d_1} \sin \beta = 2P_{B\ end} \tan \beta$$

Note that the end battens are allowed to have a different buckling load than that for the interior battens. The member loadings in the second bay from the left end are, from Eq. (1),

$$T_{d_2} = \frac{P_B - P_{B\ end}}{\cos \beta}$$

and, from Eq. (2),

$$P_{\ell_2} = 2(P_B - P_{B\ end}) \tan \beta$$

In the third bay,

$$T_{d_3} = \frac{P_{B\ end}}{\cos \beta}$$

and

$$P_{\ell_3} = 2P_{B\ end} \tan \beta$$

It is seen that, for $P_{B\ end} = P_B$ (end battens have the same properties as the others), every other bay is totally unloaded. In order that the bays be uniformly loaded, the end battens must have half the Euler buckling load of the others,

$$P_{B\ end} = \frac{1}{2} P_B$$

Then the diagonal tension in all bays is

$$T_d = \frac{P_B}{2 \cos \beta}$$

and the longeron compression in all bays is

$$P_\ell = P_B \tan \beta$$

For the BAT Beam geometry, $\beta = 45$ degrees. Thus,

$$T_d = \frac{1}{\sqrt{2}} P_B$$

and

$$P_\ell = P_B$$

The effects of inaccuracies in member lengths on load distribution are complex and require computer analysis using the finite-element approach. Experiments have shown that:

1. Increasing diagonal tension by application of external load in one bay of a similar structure (continuous-longeron Astromast) causes a decrease in diagonal tension in the two adjacent bays and alternating increase/decrease in succeeding bays. This effect dies out in about five bays either because of geometrical constraints or of longeron bending stiffness.

2. Inward deflection of a single batten frame causes alternate outward/inward deflections of succeeding batten frames in both directions. This deflection is accomplished with an applied load much less than the batten buckling load.

2.2 EFFECT OF PURE BENDING MOMENT

In Figure 2a, a pure bending moment M = 3/4 DF is applied to the beam tip by load F at Point 1a and loads -F/2 at Points 1b and 1c. Because of symmetry of the loads and the structure, the internal loads are symmetrical about the x-z plane. At Point 1a,

$$\sum F_x = 2T_{1a2b} \cos\beta \cos 30^o - 2P_{B\ end} \cos 30^o = 0$$

$$\sum F_z = P_{1a2a} - 2T_{1a2b} \sin\beta + F = 0$$

Then,

$$T_{1a2b} = \frac{P_{B\ end}}{\cos\beta}$$

and

$$P_{1a2a} = 2P_{B\ end} \tan\beta - F$$

At Point 1b,

$$\sum F_x = -T_{1b2a} \cos\beta \cos 30^o + P_{B\ end} \cos 30^o = 0$$

$$\sum F_y = T_{1b2a} \cos\beta \sin 30^o - P_{B\ end} \sin 30^o + T_{1b2c} \cos\beta - P_{B\ end} = 0$$

$$\sum F_z = P_{1b2b} - T_{1b2a} \sin\beta - T_{1b2c} \sin\beta - \frac{F}{2} = 0$$

Then,

$$T_{1b2a} = T_{1b2c} = \frac{P_{B\ end}}{\cos \beta}$$

and

$$P_{1b2b} = 2P_{B\ end} \tan \beta + \frac{F}{2}$$

For $P_{B\ end} = 1/2\ P_B$ and $\beta = 45$ degrees, the diagonal tension force is

$$T_d = \frac{1}{\sqrt{2}} P_B$$

Diagonal forces are therefore unaffected by end moment. The upper longeron compression is

$$P_{1a2a} = P_B - F$$

and the lower longeron compressions are

$$P_{1b2b} = P_{1c2c} = P_B + \frac{F}{2}$$

These longeron loads carry on through the structure, as seen by Eq. (2), so that all the upper longeron compression loads are reduced by F, and all the lower longeron compression loads are increased by F/2. Structural bending results because of elongation of the upper longeron

$$\Delta \ell_u = \ell \frac{F}{EA}$$

and of the lower longerons

$$\Delta \ell_\ell = -\ell \frac{F}{2EA}$$

These equations apply only if all longerons are in compression. For $F > P_B$, the upper longeron is in tension, and its length can increase because the joints open up. If there are no springs in the joints, then they will open abruptly to line up the hinge pins as shown in Figure 2b. The additional extension is

$$\Delta_{ct} = 2\sqrt{\left(\frac{\ell}{2}\right)^2 + (2s)^2} - \ell$$

For example, for $\ell = 78.74$ inches and $s = 0.25$ inch,

$$\Delta_{ct} = 0.00635 \text{ inch}$$

Similarly, for $F < -2P_B$, the lower longerons go into tension, and their lengths are increased by Δ_{ct}.

The longeron lengths are then given by

$$\ell_u = \ell + \Delta\ell_u = \ell\left(1 + \frac{F}{EA}\right) + \Delta_{ct}\langle F - P_B\rangle$$

and

$$\ell_\ell = \ell + \Delta\ell_\ell = \ell\left(1 - \frac{F}{2EA}\right) + \Delta_{ct}\langle -(F + 2P_B)\rangle$$

where we have used the convention

$$\langle Q\rangle = 0 \qquad \text{for } Q \text{ negative}$$

and

$$\langle Q\rangle = 1 \qquad \text{for } Q \text{ positive}$$

Actually, the center hinge on each longeron is preloaded to keep it closed. This will delay its opening until the tension gets great enough to overcome the preload. Nevertheless, because the two end hinges are on the member edge and are unpreloaded, they will tend to open, and elastic bending

of the longeron will cause axial displacement. The behavior can be predicted as follows. Let M_0 be the preload moment for the center hinge, EI be the bending stiffness of the longeron, and y be its lateral deflection. Then the equations governing the bending can be written in terms of the compression P to be

$$EI\, y'''' + Py'' = 0$$

with boundary conditions at the end hinge

$$y(0) = 0$$

$$EI\, y''(0) = Ps$$

$$EI\, y'''(0) + Py'(0) = 0$$

The boundary condition at the center hinge for tension less than that required to overcome the preload is

$$y''\left(\frac{\ell}{2}\right) = 0$$

For larger loading, the boundary condition becomes

$$EI\, y''\left(\frac{\ell}{2}\right) = -M_0 - Ps$$

The solution of these equations is

$$y = s\left[1 - \frac{\cosh \lambda \left(\frac{1}{2} - \frac{x}{\ell}\right)}{\cosh \frac{\lambda}{2}}\right], \text{ for } \lambda^2 \left(1 + \operatorname{sech} \frac{\lambda}{2}\right) < \frac{M_0 \ell^2}{EIs}$$

$$\text{or } y = s\ 1\left[- \frac{\cosh \lambda\left(\frac{1}{2} - \frac{x}{\ell}\right)}{\cosh \frac{\lambda}{2}} + \left(1 + \operatorname{sech} \frac{\lambda}{2} - \frac{M_0 \ell^2}{EIs\lambda^2}\right) \frac{\sinh \frac{\lambda x}{\ell}}{\sinh \frac{\lambda}{2}} \right] ,$$

$$\text{for } \lambda^2 \left(1 + \operatorname{sech} \frac{\lambda}{2}\right) > \frac{M_0 \ell^2}{EIs}$$

where

$$\lambda^2 = - \frac{P\ell^2}{EI}$$

The increase in length due to this combined joint opening and bending for both half longerons is

$$\Delta_{ct} = 2 \left\{ s\left[y'(0) + y' \frac{\ell}{2}\right] - \frac{1}{2} \int_0^{\ell/2} (y')^2 dx \right\}$$

Substituting for the deflections gives

$$\Delta_{ct} = \left[\frac{2s^2\lambda}{\ell} \frac{\sinh \frac{\lambda}{2}}{\cosh \frac{\lambda}{2}} - \frac{1}{8} \frac{\sinh \lambda - \lambda}{\cosh^2 \frac{\lambda}{2}} \right.$$

$$+ B \left(\frac{1 + \cosh \frac{\lambda}{2}}{\sinh \frac{\lambda}{2}} - \frac{1}{4} \frac{\lambda}{\cosh \frac{\lambda}{2}} \right)$$

$$\left. - B^2 \left(\frac{1}{8} \frac{\sinh \lambda + \lambda}{\sinh^2 \frac{\lambda}{2}} \right) \right]$$

where

$$B = 1 + \operatorname{sech} \frac{\lambda}{2} - \frac{M_0 \ell^2}{EIs\lambda^2}$$

Note that the terms containing B should be neglected if B is negative.

These equations can be used to replace Δ_{ct} in the previous equations for ℓ_u and ℓ_ℓ.

The resulting radius of curvature of the beam is

$$R = \frac{3}{4} D \frac{\ell}{\ell_u - \ell_\ell}$$

The tip deflection of a beam of length L is given by

$$\Delta_{tip} = \frac{L^2}{2R}$$

Setting $L = n\ell$ and substituting for R gives

$$\Delta_{tip} = \frac{2}{3} \frac{n^2 \ell (\ell_u - \ell_\ell)}{D}$$

where n is the number of bays.

Figure 2c shows the tip deflection Δ_{tip} as a function of tip bending moment M for a hypothetical beam of 10 bays. Beam properties are listed in Table 1. Because of Euler buckling of the longerons, applied moments are limited to the range

$$-\frac{3}{4} D \left(P_{Eu\ell} - P_\ell\right) < M < \frac{3}{4} D (2) \left(P_{Eu\ell} - P_\ell\right)$$

or for the beam of Table 1,

-2571 in-lb $< M <$ 5143 in-lb

Load-deflection curves are shown for unsprung midhinges and for the case where midhinges require 1.25 in-lb for opening. The added effective linear range due to the center moment is evident.

2.3 EFFECT OF PURE TORSION

In Figure 3, a pure torsional moment M_{tors} = 1/2 FD is applied to the end of the beam by loads F/3 acting circumferentially at each of the three corners. Rotational symmetry indicates that the internal load distributions are the same at each corner. At Point 1b,

$$\sum F_x = P_{B\ end} \cos 30^o - T_{1b2a} \cos \beta \cos 30^o + \frac{F}{3} \cos 30^o = 0$$

$$\sum F_y = -P_{B\ end} \sin 30^o - P_{B\ end} + T_{1b2a} \cos \beta \sin 30^o + T_{1b2c} \cos \beta + \frac{F}{3} \sin 30^o = 0$$

$$\sum F_z = P_{1b2b} - T_{1b2a} \sin \beta - T_{1b2c} \sin \beta = 0$$

Noting again that $P_{B\ end}$ = 1/2 P_B and β = 45 degrees, we can reduce these equations to

$$T_{1b2a} = \frac{P_B}{\sqrt{2}} + \frac{\sqrt{2}\,F}{3}$$

$$T_{1b2c} = \frac{P_B}{\sqrt{2}} - \frac{\sqrt{2}\,F}{3}$$

$$P_{1b2b} = P_B$$

This load distribution continues unchanged down through the structure. It is seen then that longeron compression is unaffected by pure torsion, while diagonal tensions are changed. It is noted that, for $|F| > 3/2\ P_B$ or $|M| > 3/4\ P_B D$ = 750 in-lb, half of the diagonals lose tension. Thus, for the beam described in Table 1, pure torsion is limited to the range

$$-750 \text{ in-lb} < M_{tors} < 750 \text{ in-lb}$$

2.4 EFFECT OF LATERAL END LOAD

In Figure 4, a radially-directed load F is applied at Point 1a. Symmetry is assumed about the x-z plane. At Point 1a,

$$\sum F_x = 2T_{1a2b} \cos\beta \cos 30^o - 2P_{B\ end} \cos 30^o + F = 0$$

$$\sum F_z = P_{1a2a} - 2T_{1a2b} \sin\beta = 0$$

At Point 1b,

$$\sum F_x = -T_{1b2a} \cos\beta \cos 30^o + P_{B\ end} \cos 30^o = 0$$

$$\sum F_y = T_{1b2a} \cos\beta \sin 30^o - P_{B\ end} \sin 30^o + T_{1b2c} \cos\beta - P_{B\ end} = 0$$

$$\sum F_z = P_{1b2b} - T_{1b2a} \sin\beta - T_{1b2c} \sin\beta = 0$$

These equations reduce to

$$P_{1a2a} = P_B - \frac{2F}{\sqrt{3}}$$

$$T_{1a2b} = T_{1a2c} = \frac{P_B}{\sqrt{2}} - \sqrt{\frac{2}{3}} F$$

$$P_{1b2b} = P_{1c2c} = P_B$$

$$T_{1b2c} = T_{1c2b} = \frac{P_B}{\sqrt{2}}$$

$$T_{1b2a} = T_{1c2a} = \frac{P_B}{\sqrt{2}}$$

A lateral load at the tip is limited to the range $-\sqrt{3}\ P_B < F < \sqrt{3/2}\ P_B$. Outside of this range, certain diagonals are slack.

The longeron loads increase along the beam, and at bay n, the change in compression for the tensioned longeron is $-2/\sqrt{3}\ nF$, and for the two compressed longerons is $1/\sqrt{3}\ nF$. Limiting the total compression in each longeron to the longeron Euler load yields the allowable range

$$-\frac{\sqrt{3}}{2n}(P_{Eu} - P_B) < F < \frac{\sqrt{3}}{n}(P_{Eu} - P_B)$$

These limits for the point design indicated in Table 1 are illustrated in Figure 4. It is seen that, for more than seven bays, Euler buckling of the longerons in the base bay defines the lateral load limit; for less than seven bays, diagonal slackening occurs before Euler buckling for loads directed toward the beam. In the general case, longeron stiffness limits loading in long beams, while batten stiffness (as it affects diagonal preload) limits loading in short beams.

SECTION 3
DEPLOYMENT AND RETRACTION

The deployment and retraction mechanism (henceforth referred to as the "deployer") is illustrated in Figures 5 through 9. As indicated in Figure 5, the deployer is itself deployable so that, in the packaged condition, it has a minimum height of either the stack height (for beams of 79 m or longer lengths) or about 2.2 m (for shorter beams) which is 10 percent greater than one bay length. The deployer uses three lead screw drives shown in Figure 6 to move the beam in and out. In the fully packaged condition, each lead screw is threaded in a stack of the open nut fittings which form part of the corner joint assemblies. The first operation consists of rotating the lead screws until the deployable portion of the three columns locks in the extended position. At this time, the top fittings on the beam will be engaged with the bottom ends of the lead screws. The three lead screws are then moved inward in order to buckle the top batten. For this task, the bearing mounts to which the lead screws are attached are movable by wormgear drive.

The deployment sequence from this point on is continuous with the lead screws lifting the mast and the longerons of the deploying bay unfolding while the diagonals extend telescopically. The batten frame which is being lifted by the lead screw is in the compressed state; that is, the battens are buckled. Before the next batten frame can thread into the lead screws, it must also be compressed.

3.1 BATTEN COMPRESSION

Since the natural batten state in the deployed beam is compressed, it is possible for the beam itself to perform this function. The longeron midhinges, which are moment-generating, can drive each bay toward deployment and thus compress the battens. In Section 2.1, it was shown that the longeron preload is equal to twice the end batten buckling load ($P_{\ell} = 2P_{B\ end}$). In Figure 10, the bay geometry is shown just prior to batten compression when the upper batten frame is compressed, the lower batten is straight, the diagonals are nominally taut, and the longerons are still folded. Point A on the lower

batten frame is at $x = r + \delta$, $y = 0$, and $z = 0$. Point B on the upper frame is at $-r/2, \sqrt{3}/2\ r, s$. The distance between them is

$$d = \sqrt{3r^2 + \ell^2} = \sqrt{\left(\frac{3}{2} r + \delta\right)^2 + \frac{3}{4} r^2 + s^2}$$

Then,

$$3r^2 + \ell^2 = \frac{9}{4} r^2 + 3r\delta + \delta^2 + \frac{3}{4} r^2 + s^2$$

$$= 3r^2 + 3r\delta + \delta^2 + s^2$$

or

$$s^2 = \ell^2 - 3r\delta - \delta^2$$

$$= (78.740)^2 - 3\left(\frac{78.74}{\sqrt{3}}\right)(0.1) \cos 30^\circ - (0.1 \cos 30)^2$$

$$s = 78.665 \text{ in.}$$

The longeron fold angle is

$$\theta = \cos^{-1} \frac{78.665}{78.740} = 2.50^\circ$$

The required midhinge moment for unassisted deployment is

$$M_{req} = \frac{\ell}{2} 2P_B \sin \theta$$

$$= (78.74 \text{ in.})\ (11 \text{ lb}) \sin 2.50^\circ$$

$$= 37.8 \text{ in-lb}$$

Such a moment is difficult to achieve. A spring along the member centerline acting about a hinge pin on the member edge, must be loaded to

$$F_{req} = \frac{M_{req}}{\frac{1}{2} d_{\ell}} = \frac{37.8 \text{ in-lb}}{\frac{1}{2} (0.5 \text{ in.})} = 151 \text{ lb}$$

in order to produce this moment. A suggested hinge for generating this moment is shown in Figure 11. Note that a linkage is used to produce a large amplification of spring torque.

3.2 MECHANISMS

Only fully erected bays can be allowed to enter the lead screw. This is ensured by requiring that each batten frame pass through an escapement mechanism. The force required for passage would be sufficient to prevent an undeployed bay from passing, but not so great that the longeron precompression load is relieved. In the fully-deployed beam, where batten compression is supported by tensioned diagonals above and below each batten, the longeron preload is 11 pounds. During deployment, batten commpression is supported only by diagonals in the deployed bay above, so that they are loaded at twice their operating preload. Therefore, longeron preload at the deployer during deployment is twice the operating level, or 22 pounds.

The bottom of the lead screws are tapered to guide the open nut fittings. At other places along each lead screw, gaps are necessary for gear engagement, for support, and for longeron folding during retraction. The top end of each lead screw is also tapered to aid retraction.

3.3 ANALYSIS

3.3.1 Lead Screw Torque

In Figure 12, a section of the lead screw is shown with the open nut corner fitting to which members hinge. The lead screw can be considered to be a ramp of angle $\theta = \tan^{-1} (p/2\pi r_p)$ on which the nut rides. Four forces act on the nut:

- Vertical load L through longeron compression
- Counter-rotating force $F = \tau / r_p$
- Normal force N
- Friction force μN

Balancing vertically and horizontally yields

$$N (\cos \theta - \mu \sin \theta) - L = 0$$

$$F - N (\sin \theta + \mu \cos \theta) = 0$$

Eliminating N,

$$\frac{F}{L} = \frac{\tan \theta + \mu}{1 - \mu \tan \theta} = \tan \theta + \mu$$

For a 1/2-10 stainless-steel acme-thread lead screw acting against a stainless-steel nut

$$\tan \theta = \frac{p}{2\pi r_p} = \frac{0.1}{\pi(0.46)} = 0.069$$

and

$$\mu = 0.13$$

so that

$$\frac{F}{L} \simeq 0.20$$

The lead screw torque is

$$\tau = F r_p = 0.2 L r_p$$

The vertical load F is limited to the longeron Euler buckling load (see Table 1):

$$L_{max} = 48.7 \text{ pounds}$$

Then the lead screw maximum torque is

$$\tau = (0.2)\ (48.7)\ (0.23)$$

$$= 2.24 \text{ in-lb}$$

3.3.2 Support Spacing

There are two criteria for determining lead screw support spacing: deformation due to side load and whirl. Side load is limited to

$$W = 2\ P_B \cos 30^0 = \sqrt{3}\ P_B = 19.05 \text{ pounds}$$

Using a conservative approach which assumes that the lead screw between support points acts as a simply supported beam, we find the maximum center deflection to be

$$y_{max} = \frac{Ws^3}{48\ EI}$$

where s is the distance between supports and W is the load. The lead screw bending stiffness is

$$EI = E\ \frac{\pi}{4}\ r^4 = (30 \times 10^6 \text{ psi})\ \frac{\pi}{4}\ (0.185 \text{ in.})^4$$

$$= 27{,}300 \text{ lb-in}^2$$

The maximum allowable spacing is

$$s = \left(\frac{48\ EI\ y_{max}}{W}\right)^{1/3}$$

If y_{max} is made less than 0.1 cos 30^{o} inch, so that the battens remain buckled,

$$s = \left[\frac{(48)(27,300)(0.0866)}{19.05}\right]^{1/3}$$

$$= 18.1 \text{ inches}$$

Four equally spaced supports at s = 15.75 inches separation, results in a maximum deflection of y_{max} = 0.058 so that the battens indeed remain buckled.

3.3.3 Whirl

The lead screw, thus designed with a span length s, has a natural flexural frequency of

$$f = 1.56 \sqrt{\frac{EI\ g}{ws^4}}$$

The linear weight of the lead screw is

$$w = \pi r_p^2 = \pi\ (0.225 \text{ in.})^2\ (0.28 \text{ lb/in}^3)$$

$$= 0.0445 \text{ lb/in}$$

Then the natural frequency is

$$f = 97 \text{ Hz}$$

In order to avoid shaft whirl, the rotational speed of the lead screws must be less than this frequency. The corresponding maximum deployment rate is 9.7 in/sec, or one bay per 8.1 sec.

3.3.4 Deployment Load Analysis

There are two conditions during deployment of a bay: 1) The compressed batten frame held by the lead screws has undeployed members below it, and 2) a completely erected bay has formed below the battem frame held by the lead screws. These cases are fundamentally different in that the load distributions below the batten frame in the lead screws differ. The vertical loads on the lead screws are not affected; in any case, they are determined by externally applied loads.

3.3.4.1 FIRST CASE

In Figure 13, the batten frame held by the lead screws has a fully deployed beam above it and a partially deployed bay below it. The longerons and diagonals of this partially deployed bay are unloaded, and the lower batten frame is unbuckled. At point A, equilibrium of forces yields

$$\sum F_x = -2P_B \cos 30^o + \left(T_{d_1} + T_{d_2}\right) \cos\beta \cos 30^o + F_x = 0$$

$$\sum F_y = \left(T_{d_1} - T_{d_2}\right) \cos\beta \sin 30^o + F_y = 0$$

and

$$\sum F_z = \left(T_{d_1} + T_{d_2}\right) \sin\beta - P_{\ell_1} + F_z = 0$$

Deployer loads are then the negative of those on the beam

$$F_{depl_x} = \frac{1}{2}\sqrt{\frac{3}{2}}\left(T_{d_1} + T_{d_2}\right) - 3P_B$$

$$F_{depl_y} = \frac{\sqrt{3}}{4}\left(T_{d_1} - T_{d_2}\right)$$

$$F_{depl_z} = \frac{1}{\sqrt{2}}\left(T_{d_1} + T_{d_2}\right) - P_{\ell_1}$$

Limiting conditions are as follows. For F_{depl_x}, with bending moment or lateral end load,

$$T_{d_1} = T_{d_2} = 0$$

or

$$T_{d_1} = T_{d_2} = \sqrt{2}\, P_B$$

In either case, some diagonals are slack. Then,

$$-19.05 \text{ lb} < F_{depl_x} < 0$$

For F_{depl_y}, with torsion,

$$-6.74 \text{ lb} < F_{depl_y} < 6.74 \text{ lb}$$

For F_{depl_z}, with bending moment or lateral end load,

$$-37.71 \text{ lb} < F_{depl_z} < 75.42 \text{ lb}$$

3.3.4.2 SECOND CASE

At point B of Figure 14, a fully deployed bay extends below. Equilibrium of forces yields

$$\sum F_x = -2P_B \cos 30^\circ + \left(T_{d_1} + T_{d_2} + T_{d_3} + T_{d_4}\right) \cos\beta \cos 30^\circ + F_x = 0$$

$$\sum F_y = \left(T_{d_1} - T_{d_2} + T_{d_3} - T_{d_4}\right) \cos\beta \sin 30^\circ + F_y = 0$$

$$F_z = \left(T_{d_1} + T_{d_2} - T_{d_3} - T_{d_4}\right) \sin \beta + P_{\ell_1} - P_{\ell_2} + F_z = 0$$

Deployer loads are then

$$F_{depl_x} = \frac{1}{2}\sqrt{\frac{3}{2}}\left(T_{d_1} + T_{d_2} + T_{d_3} + T_{d_4}\right) - \sqrt{3}\, P_B$$

$$F_{depl_y} = \frac{\sqrt{3}}{4}\left(T_{d_1} - T_{d_2} + T_{d_3} - T_{d_4}\right)$$

$$F_{depl_z} = P_{\ell_1} - P_{\ell_2} - \frac{1}{\sqrt{2}}\left(T_{d_1} + T_{d_2} - T_{d_3} - T_{d_4}\right)$$

Limiting conditions are as follows. For F_{depl_x}, with bending moment or lateral end load,

$$T_{d_1} = T_{d_2} = 0; \quad T_{d_3} = T_{d_4} = \sqrt{2}\, P_B$$

or

$$T_{d_1} = T_{d_2} = T_{d_3} = T_{d_4} = \sqrt{2}\, P_B$$

$$0 \leqq F_{depl_x} \leqq 19.05 \text{ lb}$$

For F_{depl_y}, with torsion,

$$-6.74 \text{ lb} \leqq F_{depl_y} \leqq 6.74 \text{ lb}$$

For F_{depl_z}, with bending moment or lateral end load,

$$-37.71 \text{ lb} \leqq F_{depl_z} \leqq 75.42 \text{ lb}$$

Thus, depending on external loading and on whether or not a bay has deployed within the deployer, radial loads required of the deployer can be as high as 19.05 pounds inward or outward, circumferential loads can be 6.74 pounds in either direction, and vertical loads can be as great as 37.71 pounds pushing up on a longeron or 75.42 pounds pulling on one.

3.4 COST

Costs of design and manufacture of an engineering model of the BAT Beam deployer/retractor may be estimated as follows. Thermal considerations concerning relative lengths of a single bay (2 m) and of the lead screw dictate that the deployer should be stainless steel having a low coefficient of thermal expansion. The level of effort should be sufficient for a thorough understanding of deployment and retraction, short of the special requirements of actual flight (redundancy, etc.).

This effort includes:

- Engineering for stress and geometrical analyses, thermal analysis, management of design, manufacturing, and assembly - 700 hours
- Design for detailed drawings of approximately 20 components - 600 hours
- Manufacturing 60 parts - 500 hours
- Assembly of three complete corner units with synchronizing hardware - 400 hours
- Material and purchased parts - $3000

The estimated cost of this effort, including overhead and fees, is approximately $150,000.

For development and demonstration of BAT Beam deployment, an engineering model of the beam itself must also be available. It should satisfy all aspects of the BAT Beam concept in addition to interfacing with the deployer. In this respect, the corner bodies need modification to include the open nut which threads into the lead screw, as shown in Figure 9.

This effort, to make an eight-bay model, would involve the same personnel as above and would cost approximately $50,000.

Thus this effort, for a demonstration-level BAT Beam and deployer, would cost approximately $200,000 and would take approximately 8 months.

SECTION 4

INFLUENCE OF JOINT IMPERFECTIONS ON THE EFFECTIVE STIFFNESS OF A TRUSS MEMBER

Consider a properly designed butt joint in which the two ends are supposed to be in contact over their entire area. The joint is assumed to be preloaded so that incremental tension forces do not put the joint into tension. If the joint is perfectly made, it behaves as if the material were continuous through the joint; there is no additional joint compliance.

In fact, imperfections of the joint are unavoidable. The imperfections will cause additional displacements as the mating surfaces try to adjust themselves to carry changes in loading. If the preload is great enough to overcome the imperfections, then the joint can be made "perfect." Smaller amounts of preload will result in varying amounts of joint compliance. The question to be investigated is how the preload is related to the amount of imperfection and acceptable amount of joint compliance.

4.1 DOMED ENDS

Let the mismatch between the two surfaces be spherical. Then the well known work of Hertz can be used to estimate the deflections. From Reference 1, we get the displacement Δ due to local deformation of the contact surface of two spheres of radius R pressed together with a force P

$$\Delta = 1.55\left(\frac{P^2}{E^2R}\right)^{1/3}$$

Let the diameter of the joint be d. The sphericity of the mating surfaces will cause a gap of δ around the periphery equal to

$$\delta = \frac{d^2}{4R}$$

Solving for R and substituting gives

$$\frac{\Delta}{d} = 2.09\ \epsilon^{2/3} \left(\frac{\delta}{d}\right)^{1/3}$$

where

$$\epsilon = \frac{P}{\pi d^2\ E/4}$$

is the strain in the strut away from the contact surface.

The dimensionless compliance of the joint is

$$\frac{d(\Delta/d)}{d\epsilon} = 1.39 \left(\frac{\delta/d}{\epsilon}\right)^{1/3}$$

The total compliance of the strut of length ℓ and the joint is

$$C = \frac{\ell}{E_s A_s} + \frac{d}{E\pi d^2/4} \frac{d(\Delta/d)}{d\epsilon}$$

$$= \frac{\ell}{E_s A_s} + \frac{1.77}{Ed} \left(\frac{\delta/d}{\epsilon}\right)^{1/3}$$

This equation can be used to determine the prestrain ϵ (and, hence, the precompression) to keep the second term small enough. As an example, consider a strut built of graphite/epoxy tubing with titanium ends. Let the tubing have a wall thickness of 0.06 inch and let the the tubing and the joint have a diameter of 0.5 inch. Let the length ℓ be 39.37 inches. Let $E = 17 \times 10^6$ psi and $E_s = 15 \times 10^6$ psi. Then,

$$C = 31.6 \times 10^{-6} + 0.208 \times 10^{-6} \left(\frac{\delta/d}{\epsilon}\right)^{1/3} \text{ in/lb}$$

If we want to limit the joint compliance to 5 percent of the strut compliance, then the prestrain must be greater than

$$\epsilon = 2.29 \times 10^{-3}\ \delta/d$$

Let $\delta/d = 0.001$ inch. Then,

$$\varepsilon = 2.29 \text{ microinches/inch}$$

The corresponding required preload is

$$P = 7.64 \text{ pounds}$$

The accuracy of the foregoing analysis is best when the contact diameter is small in comparison to the strut diameter. The contact diameter is found from Reference 1 to be

$$d_{con} = 1.762 \left(\frac{PR}{E}\right)^{1/3}$$

Substituting for P and R gives

$$\frac{d_{con}}{d} = 1.024 \left(\frac{\varepsilon}{\delta/d}\right)^{1/3}$$

For the values in the present example

$$\frac{d_{con}}{d} = 0.107$$

which is small enough.

4.2 WAVY-EDGED TUBES

If the graphite composite tubes are butted together, the possibility is that the edges mismatch in a sinusoidal fashion. Inasmuch as the tubes are usually composed mostly of longitudinal fiber, the behavior can be approximated by means of shear-lag theory. Thus, let x be the distance around the circumference and y be the axial coordinate. The axial deflection v(x,y) must satisfy the following partial differential equation

$$E_c \frac{\partial^2 v}{\partial y^2} + G_c \frac{\partial^2 v}{\partial x^2} = 0$$

where E_c and G_c are Young's modulus and shear modulus of the composite.

Let the edge mismatch be

$$\delta(x) = \frac{\delta}{2}\left(1 - \cos\frac{2\pi x}{\lambda}\right)$$

where δ is the maximum gap and λ is the wavelength.

The solution is periodic in x with period λ. At the edge, $y = 0$, we have mixed boundary conditions. In the internal $-\lambda/2 < x < \lambda/2$, the conditions are

$$v = -\frac{\delta}{4}\left(1 - \cos^2\frac{\pi x}{\lambda}\right), \quad |x| < b\lambda$$

$$\frac{\partial v}{\partial y} = 0 \quad , \quad |x| > b\lambda$$

Note that symmetry of deformations in the upper and lower tubes is taken into account in the deflection boundary condition.

Let

$$x = \sqrt{\frac{G_c}{E_c}}\, x_1$$

$$\lambda = \sqrt{\frac{G_c}{E_c}}\, \lambda_1$$

Then the boundary value problem in the field $|x_1| < \lambda_1/2$, $y>0$ can be written

$$\nabla^2 v = 0$$

where on the boundary,

$$v(x_1 0) = -\frac{\delta}{2}\sin^2\frac{\pi x_1}{\lambda_1}, \quad |x_1| < b\lambda_1$$

$$\frac{\partial v}{\partial n} = 0$$

elsewhere.

We map the slit at $y = 0$, $|x_1| < b\lambda_1$ onto a unit circle in the w plane by the conformal mapping

$$\sin \pi b \left(w + \frac{1}{w} \right) = 2 \sin \frac{\pi z}{\lambda_1}$$

where

$$z = x_1 + iy$$

Let

$$v(x_1, y) = \mathrm{Re}\left[\Phi(z)\right]$$

On the unit circle, $w = e^{i\theta}$

$$\sin \pi b \cos \theta = \sin \frac{\pi x_1}{\lambda_1}$$

Also, the boundary condition on the slit becomes

$$\mathrm{Re}\left[\Phi(z)\right] = -\frac{\delta}{2} \sin^2 \pi b \cos^2 \theta$$

This requirement is satisfied if

$$\Phi = -\frac{\delta}{4} \sin^2 \pi b \left(1 + \frac{1}{w^2}\right) + A \ell n\, w$$

Since the transformation is singular at $w = \pm 1$, the derivative $d\Phi/dw$ must be zero there to avoid infinite stresses at the edges of the slit. The constant A is selected accordingly to give

$$\Phi = -\frac{\delta}{4} \sin^2 \pi b \left(1 + \frac{1}{w^2} + 2\, n\ell w\right)$$

Setting $z = iy$ and solving for w gives

$$w = \left(i \frac{\sinh \frac{\pi y}{\lambda_1}}{\sin \pi b} + \sqrt{1 + \frac{\sinh^2 \frac{\pi y}{\lambda_1}}{\sin^2 \pi b}} \right)$$

Substituting gives

$$v(0,y) = \frac{\delta}{2} \sin^2 \pi b \left[\frac{\sinh \frac{\pi y}{\lambda_1}}{\sin \pi b} \left(\frac{\sinh \frac{\pi y}{\lambda_1}}{\sin \pi b} - \sqrt{1 + \frac{\sinh^2 \frac{\pi y}{\lambda_1}}{\sin^2 \pi b}} \right) - \ell n \left(\frac{\sinh \frac{\pi y}{\lambda_1}}{\sin \pi b} \sqrt{1 + \frac{\sinh^2 \frac{\pi y}{\lambda_1}}{\sin^2 \pi b}} \right) \right]$$

Expanding in a series for large y gives

$$v(0,y) \cong \frac{\delta}{2} \sin^2 \pi b \left[-\frac{1}{2} - \frac{\pi y}{\lambda_1} - \ell n \left(\frac{1}{\sin \pi b} \right) \right]$$

Therefore, the compressive strain away from the edge is

$$\varepsilon = + \frac{\pi \delta}{2 \lambda_1} \sin^2 \pi b$$

and the joint displacement of the combined upper and lower struts is

$$\Delta = \frac{\lambda_1 \varepsilon}{\pi} \left[1 + \ell n \left(\frac{\frac{\delta}{2}}{\frac{\lambda_1 \varepsilon}{\pi}} \right) \right]$$

Let n be the number of full waves around the tube. Then

$$\lambda = \frac{\pi d}{n}$$

and

$$\frac{\lambda_1 \varepsilon}{\pi} = \frac{d \varepsilon}{n} \sqrt{\frac{E_c}{G_c}}$$

Therefore,

$$\frac{\Delta}{d} = \frac{\varepsilon}{n}\sqrt{\frac{E_c}{G_c}}\left[1 + \ell n\left(\frac{\delta/d}{2\ \varepsilon/n\ \sqrt{E_c/G_c}}\right)\right]$$

The dimensionless compliance is

$$\frac{d(\Delta/d)}{d\varepsilon} = \frac{1}{n}\sqrt{\frac{E_c}{G_c}}\ \ell n\left(\frac{\delta/d}{2(\varepsilon/n)\ \sqrt{E_c/G_c}}\right)$$

Including the compliance of the strut of length ℓ, the total compliance is

$$C = \frac{\ell}{E_s A_s} + \frac{d}{E_s A_s}\frac{d(\Delta/d)}{d\varepsilon}$$

Consider $E_c/G_c = 10$, $n = 2$, and $\delta = 0.001$ in for the same strut as before. The resulting required prestrain for the joint compliance to be limited to 5 percent is

$$\varepsilon = 52.4 \times 10^{-6}$$

The corresponding preload is

$$P = 74.1 \text{ pounds}$$

The portion of the circumference of the tube in contact is

$$2b = \frac{2}{\pi}\sin^{-1}\sqrt{\frac{2}{n}\frac{\sqrt{E_c/G_c}\ \varepsilon}{\delta/d}}$$

For the present example,

$$2b = 0.186$$

Of course, if ε is great enough, the entire circumference is in contact and the joint compliance becomes zero.

4.3 ANGULAR MISALIGNMENT

A third type of joint imperfection arises from the tendency of a hinged joint not to close on full deployment. The joint preload is then needed to cause the struts to bend enough to close the gap.

Let α be the angular misalignment without preload. Then the preload moment required to close the gap is

$$M_0 = \frac{2\,EI\,\alpha}{\ell}$$

where ℓ is the length of the struts on each side of the joint and EI is the bending stiffness. The other ends of the struts are assumed to be clamped.

Assume that the struts are tubular and that the preload moment is produced by a load at the center of the tube close to the joint. The prestrain produced by the preload necessary to close the joint is

$$\varepsilon = \frac{d}{2\ell}\alpha$$

As an example, let the values of d and ℓ be assumed as in the previous cases and let the gap be 0.001 inch (α = 0.002 rad). Then

$$\varepsilon = 12.7 \times 10^{-6}$$

This value is smaller than the one obtained for the wavy edge with the same maximum gap. If the struts were less slender, the values would be nearer and the interaction between strut bending and end distortion would be important. This can be readily accomplished by setting n = 1 in the wavy-edge analysis and letting

$$\frac{\delta}{d} = \alpha - \frac{2\ell}{d}\varepsilon$$

Before the joint is fully closed, the additional compliance due to the strut's bending needs to be included. The unit shortening due to this effect is

$$\frac{\Delta_b}{\ell} = \frac{y'(0)}{\ell}\frac{d}{2} + \frac{1}{2\ell}\int_0^{\ell} (y')^2\, dx$$

If beam columning is ignored, the result is

$$\frac{\Delta_b}{\ell} = \epsilon\left(\frac{1}{2} + \frac{1}{15}\,\epsilon\,\frac{\ell^2}{d^2}\right)$$

Thus the additional compliance is at least 50 percent of the nominal value. The conclusion is that the preload must be enough to close the gap. Including the effects of end distortion, the criterion becomes

$$\alpha - \frac{2\ell}{d}\,\epsilon = 2\sqrt{\frac{E_c}{G_c}}\,\epsilon$$

Thus the required preload is

$$\epsilon = \frac{\alpha}{2(\ell/d + \sqrt{E_c/G_c})}$$

4.4 COMPLIANCE OF A CENTERED-HINGE JOINT

Consider a simple hinge joint in which the axial loads are carried from one strut to another through a hinge pin in shear as shown in Figure 15.

The joint is designed to be symmetrical for ease in this preliminary analysis. Of course, actual joints tend to be asymmetrical. Note that we have assumed certain of the dimensions to be related to the outer diameter d of the tube. Variations in the joint include the pin diameter d_0, the edge thickness t, and the materials of the joint halves and the pin.

The total joint compliance is estimated to be the sum of the following sources:

1. The reduced net cross section over the length d
2. The bearing of the pin into each half (if the joint is in compression)
3. The stretching of the edge in each half (if the joint is in tension)
4. The bending of the pin

The effects of coupling between these sources are ignored. The results should yield higher compliances than are actually the case.

Each source is considered separately.

4.4.1 Reduced Net Section

The section is reduced by less than half. Assume that it is half of the original. Then, inasmuch as the length is d,

$$C_1 = \frac{8}{\pi dE}$$

4.4.2 Bearing Displacement

Assume that the pin acts as a rigid punch of width d_0. Then, for smooth contact, Milne-Thompson (Ref. 2, p. 99) gives the complex stress to be

$$W(z) = -\frac{P}{\pi} \frac{1}{\sqrt{(d_0/2)^2 - z^2}}$$

where P is the load per unit length on the punch. The integral is

$$G(z) = -\frac{P}{\pi} \sin^{-1} \frac{2z}{d_0} = \frac{iP}{\pi} \ell n \left[\sqrt{1 - \left(\frac{2z}{d_o}\right)^2} + i \frac{2z}{d_0} \right]$$

The complex displacement is

$$4\mu(u + iv) = \chi G(z) + G(\bar{z}) - (z - \bar{z}) \bar{W}(\bar{z})$$

On the y axis, z = iy

$$W(z) = -\frac{P}{\pi}\frac{1}{\sqrt{(d_0/2)^2 + y^2}}\left|\frac{y}{y}\right|$$

$$G(z) = \frac{iP}{\pi}\ln\sqrt{1 + \frac{2y^2}{d_0}} - \frac{2|y|}{d_0}$$

The displacement in the y direction is

$$v = \frac{(\chi + 1)}{4G}\frac{P}{\pi}\ln\left[\sqrt{1 + \left(\frac{2y}{d_0}\right)^2} - \frac{2y}{d_0}\right] - \frac{2P}{4G\pi}\frac{y}{\sqrt{(d_0/2)^2 + y^2}}$$

Since v = 0 at y = 0, an estimate of the compliance in bearing can be obtained by setting y equal to the length d/2 of the tang. Thus, since $\chi = (3-\nu)/(1+\nu)$ $G = E/2(1+\nu)$, and the width of the tang is d/2,

$$C_2 = \frac{4}{\pi E d}\left[\ln\left(\sqrt{1 + \frac{d^2}{d_0^2}} + \frac{d}{d_0}\right) + \frac{1 + \nu}{2}\frac{1}{\sqrt{1 + d_0^2/d^2}}\right]$$

4.4.3 Edge Stretching

Assume the edge to be a band of length $\pi(d_0+t)$, width d/2, and thickness t. The tension in the band would be T/2. The strain energy is

$$\frac{\pi(d_0 + t)}{2E}\left(\frac{T/2}{dt/2}\right)^2$$

The work done by the applied load during the displace δ is $T\delta/2$. Thus, the compliance is

$$C_3 = \frac{\pi}{2E}\frac{d_0 + t}{dt}$$

4.4.4 Pin Bending

Consider the pin to be loaded as shown in the following sketch.

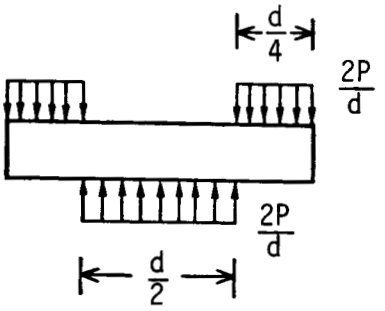

Let the compliance be estimated as the differential deflection of the centers of the loaded areas. The displacement can be found by assuming the pin to be cantilevered at the center and loaded as follows.

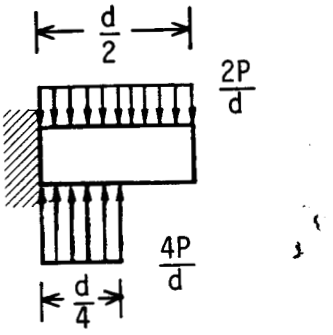

The deflection is (from Ref. 1, p. 98)

$$y = -\frac{4P}{d}\frac{1}{24EI}\left(\frac{d}{8}\right)^3\left(\frac{10}{8}\right)d + \frac{2P}{d}\frac{3}{24EI}\left(\frac{3d}{8}\right)^4 + \frac{2P}{8}\frac{(3d/8)^3}{3EI} + \frac{P}{8}\frac{d}{16}\frac{(3d/8)^2}{2EI}$$

$$= \frac{Pd^3}{EI}(-0.000407 + 0.004944 + 0.004394 + 0.00055)$$

$$= 0.0103\frac{Pd^3}{EI}$$

Therefore, the compliance is

$$C_4 = 0.659 \frac{1}{\pi d E_p} \left(\frac{d}{d_0}\right)^4$$

where E_p is the pin-material modulus. Note that this estimate is probably very conservative.

4.4.5 Numerical Example

Let d = 0.5 inch, t = d_0 = 0.1 inch, E = 17 x 10^6 psi, and E_p = 29 x 10^6 psi. Then we get

$C_1 = 0.300 \times 10^{-6}$ in/lb

$C_2 = 0.444 \times 10^{-6}$ in/lb

$C_3 = 0.370 \times 10^{-6}$ in/lb

$C_4 = 9.04 \times 10^{-6}$ in/lb

Clearly, the pin bending dominates the estimates.

Note that the compliance of a 1-m-long tube is 31.6 x 10^{-6} in/lb. If we wanted each half joint to add only 5 percent, then the total joint compliance would have to be reduced to 3.2 x 10^{-6} in/lb. This could be accomplished by using a larger pin.

4.5 COMPARISON OF JOINT COMPLIANCES

The joint compliances estimated herein are compared in Figure 16. The results are shown in nondimensional form with the nominal extensional stiffness of the joint parent material and the diameter used as dimensions of force and length, respectively.

The results for domed ends (dashed lines) and those for wavy tube ends (solid lines) are plotted versus the preload strain for three values of the imperfection parameter δ/d ranging from 10^{-4} (high) precision to 10^{-2} (rough). Note that the curves for wavy ends are cut off at the preload necessary to close a tilted end for a strut slenderness of ℓ/d = 78.74.

Also shown in Figure 16 is the compliance of the centered hinge joint for three values of pin diameter. The material properties assumed are the same as those in the preceding section, and the edge thickness is equal to the pin diameter.

The comparisons show that letting the tube ends butt together gives the least compliance of all designs, provided sufficiently high preloads are applied to remove any joint tilt. They also show that the centered hinge joint is potentially of low compliance for pin diameters greater than about 30 percent of the strut diameter.

SECTION 5
STRUCTURAL ASSESSMENT AND SUMMARY

It is recommended that the BAT Beam be used in light load applications; that is, where there is no relieving of longeron compressure or diagonal tensile preload. In this restricted-loading region, beam properties are highly favorable in terms of stiffness, because of the elimination of "deadband" by preloading. The member properties must be specified according to beam requirements, as differing load configurations have differing and in some cases exclusive effects on the members. For instance, it was shown previously that torsional loads do not affect longeron loading, and diagonal loading is not affected by bending moment.

5.1 LONGERONS

The longerons, because they are simply hinged by parallel pins, are not strained when packaged or during deployment and can then be constructed as stiff or desired for beam stiffness. It is recommended, however, that midhinges be of the type introduced in Section 3.1 and that the longeron ends are also preloaded. The midhinges have two purposes: 1) aid in deployment, so that batten compressionn is accomplished by longeron unfolding, and 2) extend full stiffness range, so that relieving longeron preload does not lengthen the member. Preloading the end hinges, which are off the member centerline, also extends full stiffness into the region where longeron compressive preload is relieved.

Without end preloading, such longeron tension reacted by the off-axis pin causes member bending which lengthens the member.

5.2 DIAGONALS

The diagonals of the BAT Beam are necessarily in pairs (two per face per bay) and are in tension. For packaging, they are designed to telescope. Non-telescoping diagonals would either protrude from the package or interfere with the packaged longerons unless the bay length were made much shorter. A

hinging cluster is required where the diagonals intersect. The problem which may arise here is diagonal lockup during beam retraction, unless some means is provided to maintain synchronization of the re-telescoping diagonals.

5.3 BATTENS

The purpose of the battens is to preload the beam. Lesser or greater values of preload are obtained by changing the batten stiffness, either by changing its cross section or material. In the example beam of Table 1, the batten material is fiberglass/epoxy while the remainder of the beam is graphite/epoxy. This material difference may not be adivsable in terms of thermal stability.

Increased preload due to increased batten stiffness also results in a greater required longeron midhinge moment in order to deploy the beam.

5.4 SUMMARY AND CONCLUSIONS

The BAT Beam is expected to be of high stiffness under loading conditons which do not relieve the preload. Use of preloaded hinges at all locations of longeron folding will extend the region of high-bending stiffness. Torsional stiffness is limited in range by diagonal preload, and can be extended by increasing the batten stiffness.

Special requirements which should be noted about the beam are 1) that the tip battens must be of half-stiffness for properly distributed preload, and 2) that the longeron midhinges must generate a moment sufficient to deploy a bay. These conditons were noted previously in Sections 2.1 and 3.1

REFERENCES

1. Roark, Raymond J.; and Young, Warren C.: Formulas for Stress and Strain. 5th Ed., McGraw-Hill Book Company, San Francisco, CA, 1975.

2. Milne-Thompson, L.M.: Plane Elastic Systems. Springer-Verlag, 1960.

TABLE 1. LENGTHS AND PROPERTIES

PARAMETER	LONGERON	BATTEN	DIAGONAL
E (psi)	15×10^6	5×10^6	15×10^6
Outside diameter (in.)	0.500	See Fig. 1	0.270
Wall (in.)	0.060	See Fig. 1	0.030
Area (in^2)	0.083	0.138	0.023
EA (lb)	1.245×10^6	6.88×10^5	3.45×10^5
I (in^4)	2.04×10^{-3}	1.38×10^{-3}	
EI (lb in^2)	3.06×10^4	6.91×10^3	
P_{Eu} (lb)	48.71	11.0	
Length (in.)	78.74	78.74	111.36
Deformation amplitude (in.)		2.54	
End shortening (in.)		0.2	

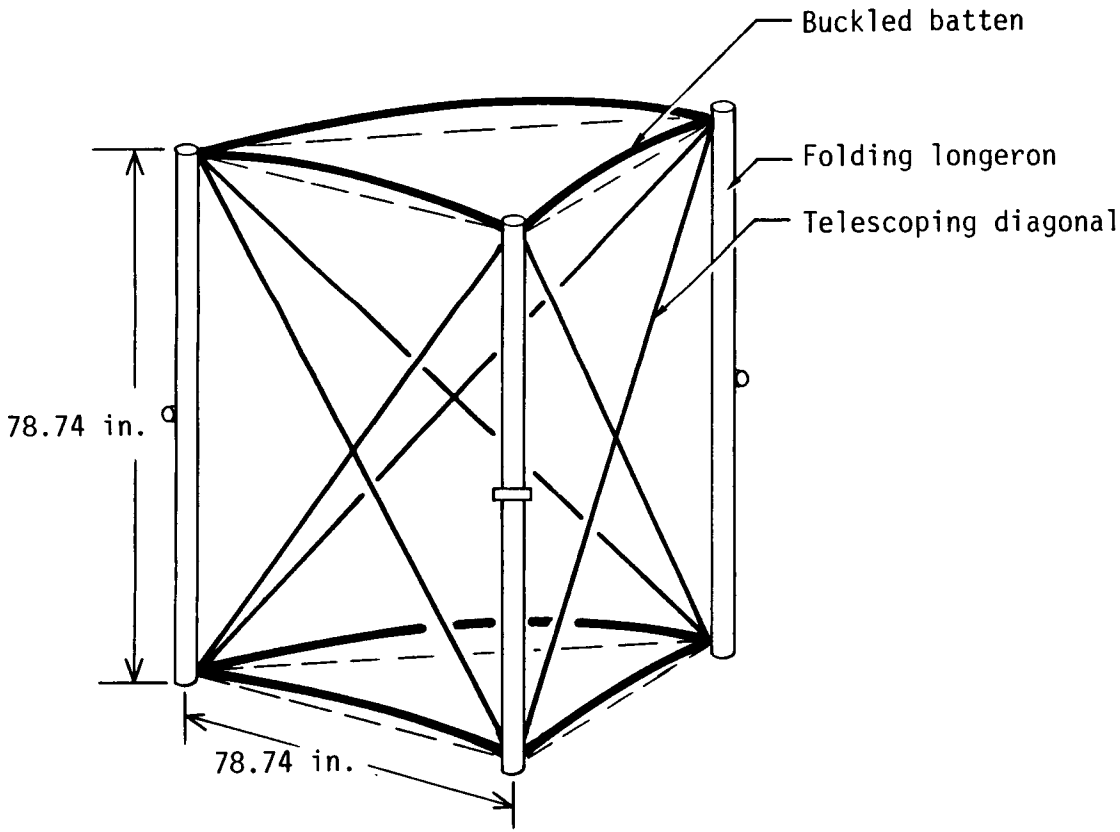

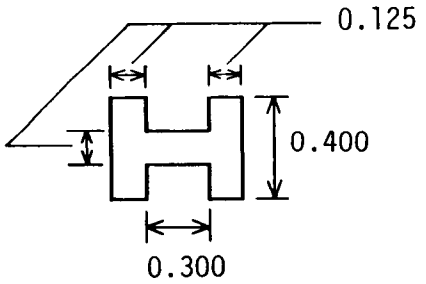

Batten cross section

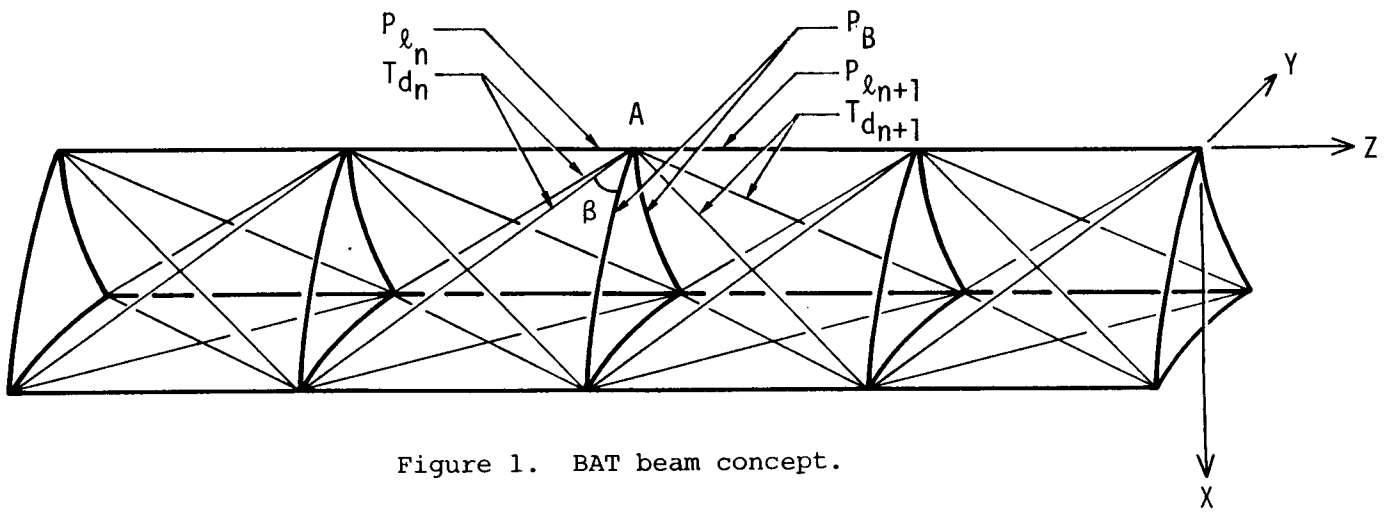

Figure 1. BAT beam concept.

126A

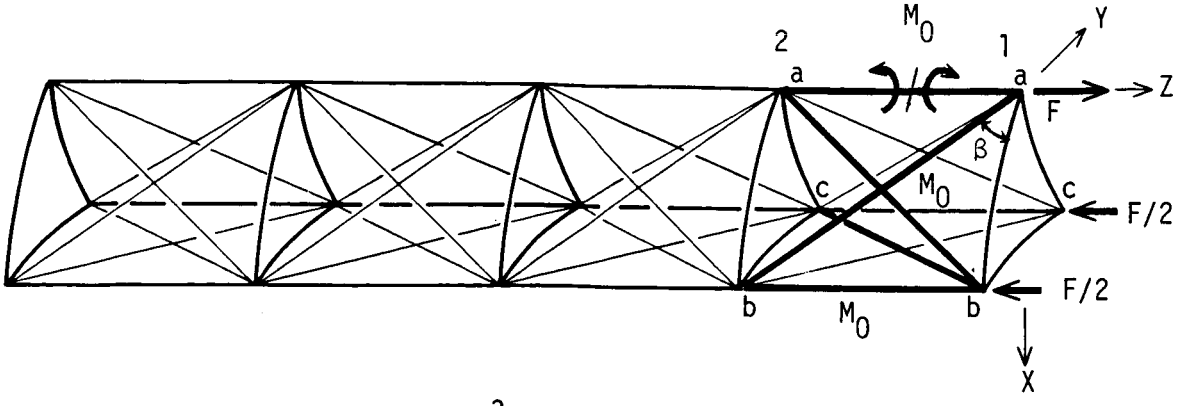

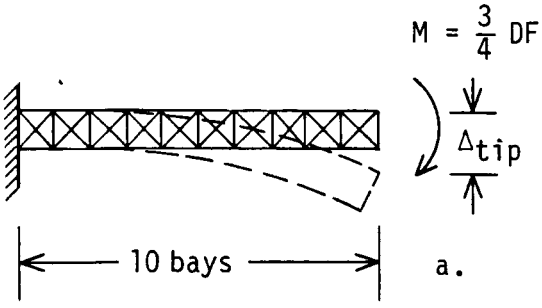

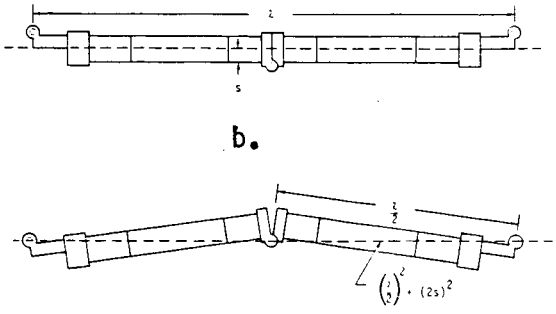

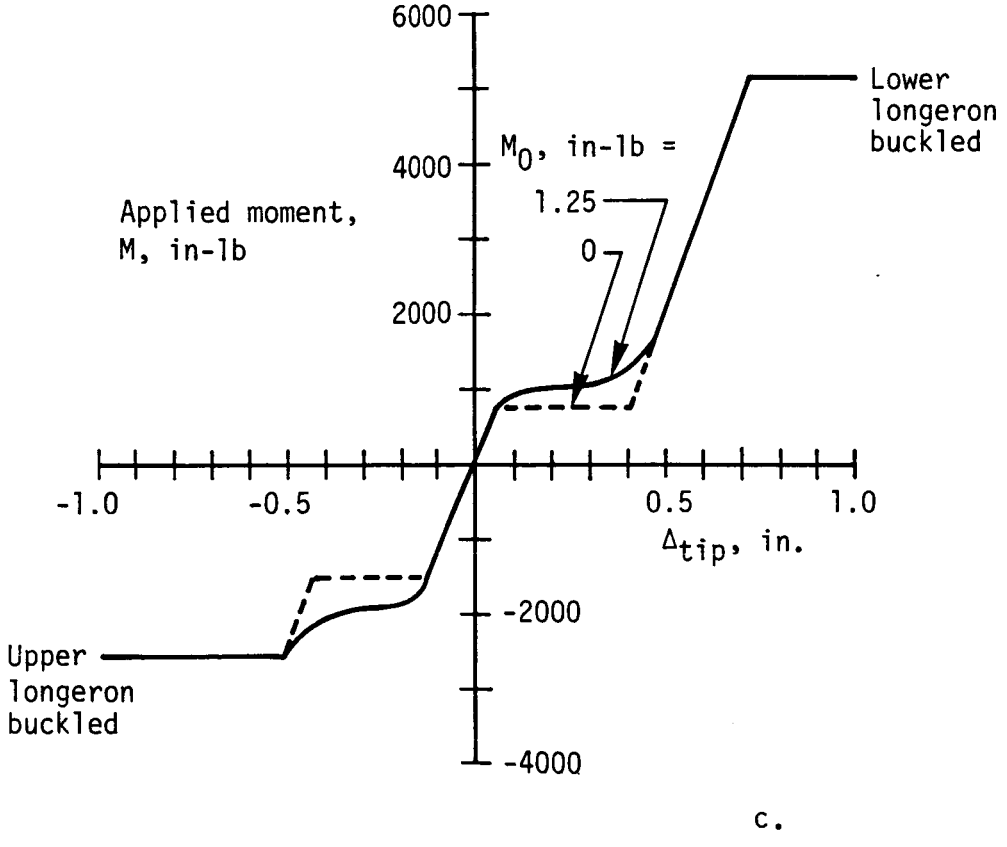

Figure 2. Pure bending moment. *127A*

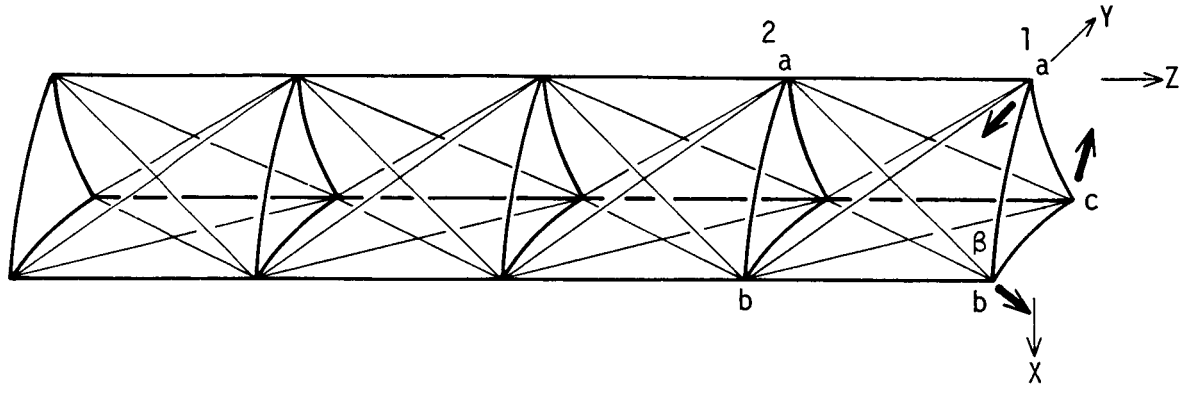

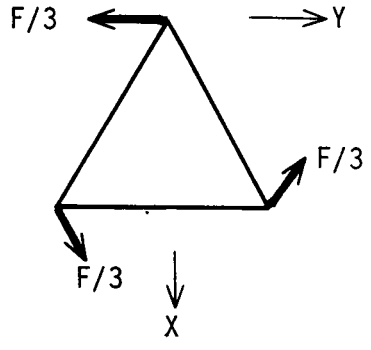

Figure 3. Pure torsion.

128A

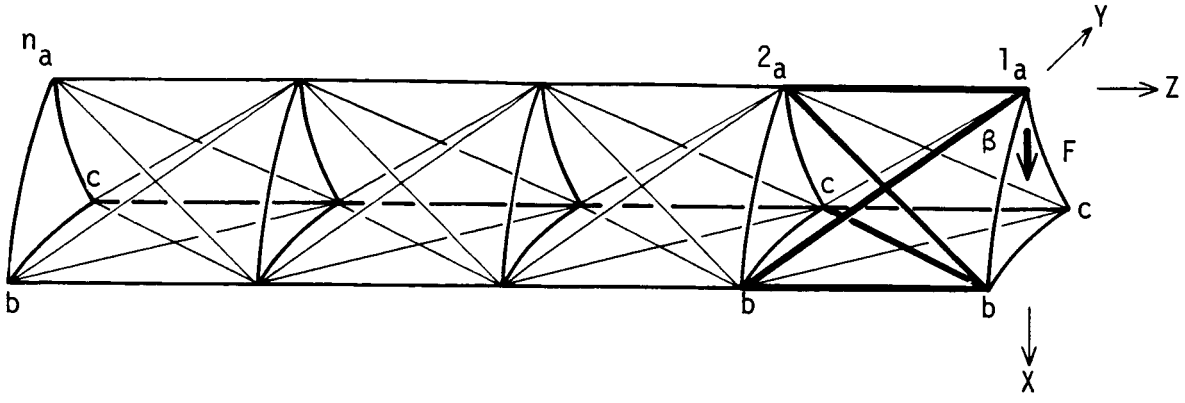

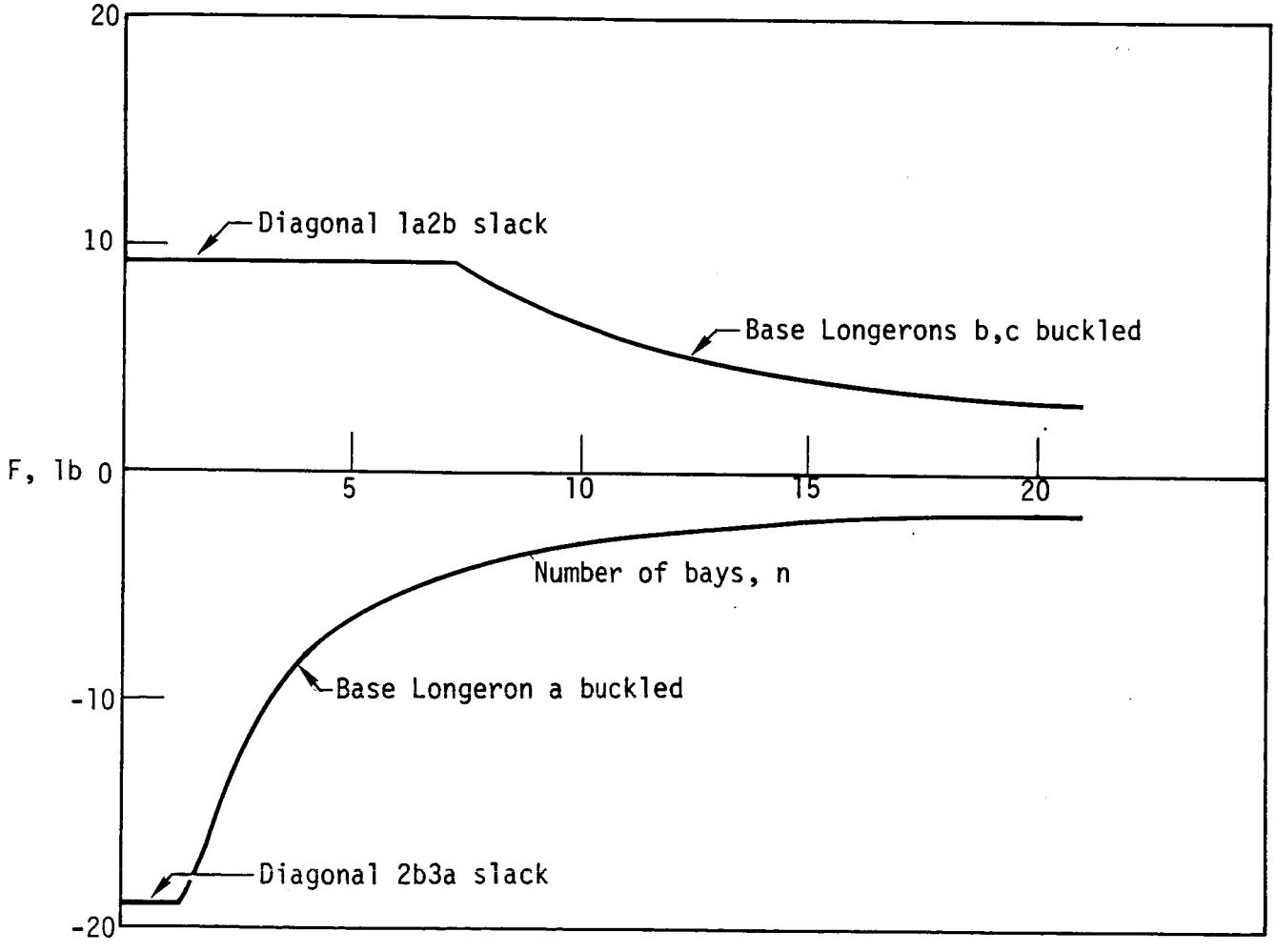

Figure 4. Effect of lateral end load. *154A*

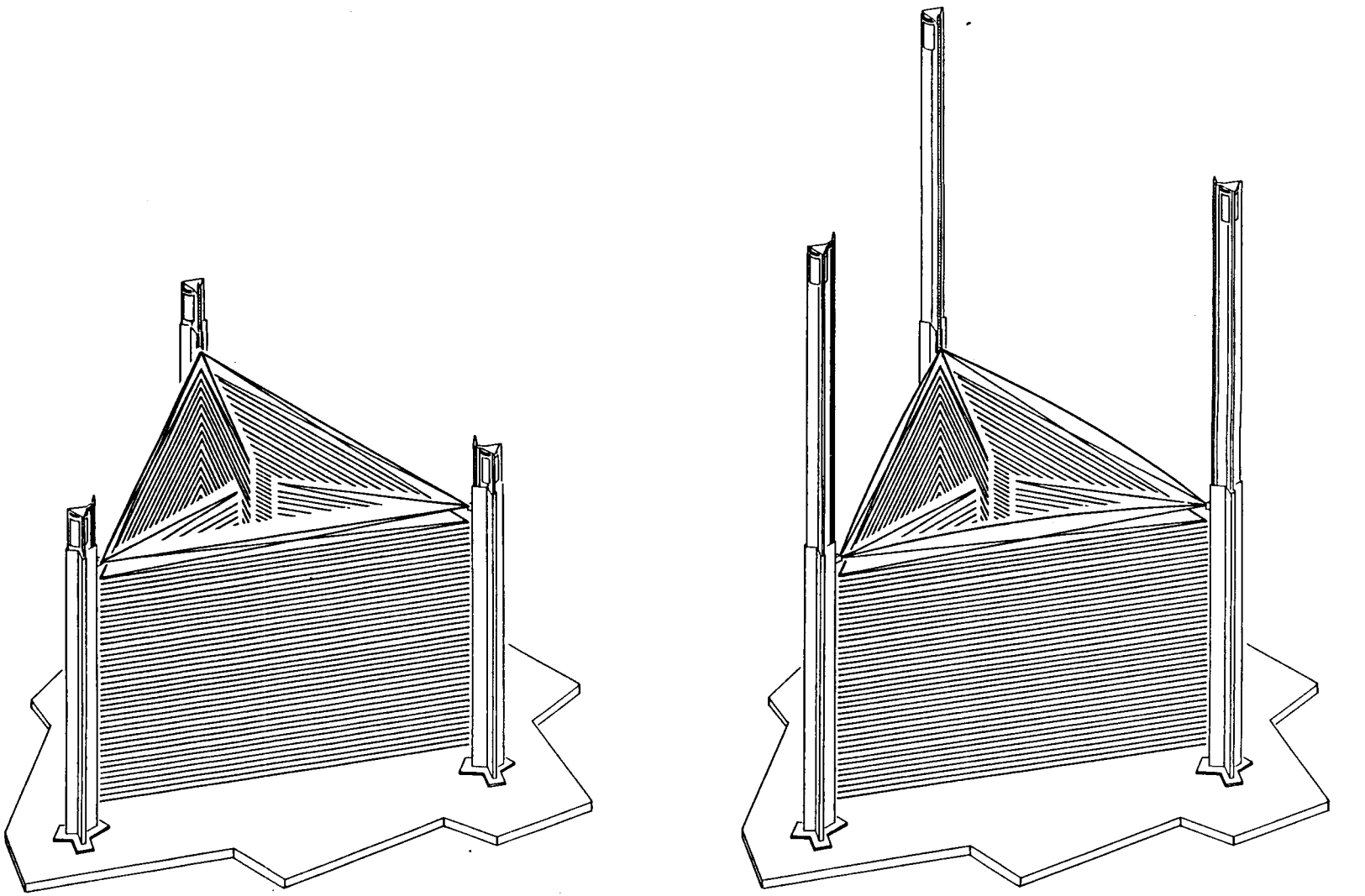

a. Launch configuration *149-1B*

b. Deployed, ready to extend beam *149-B*

Figure 5. Deployable BAT Beam deployer.

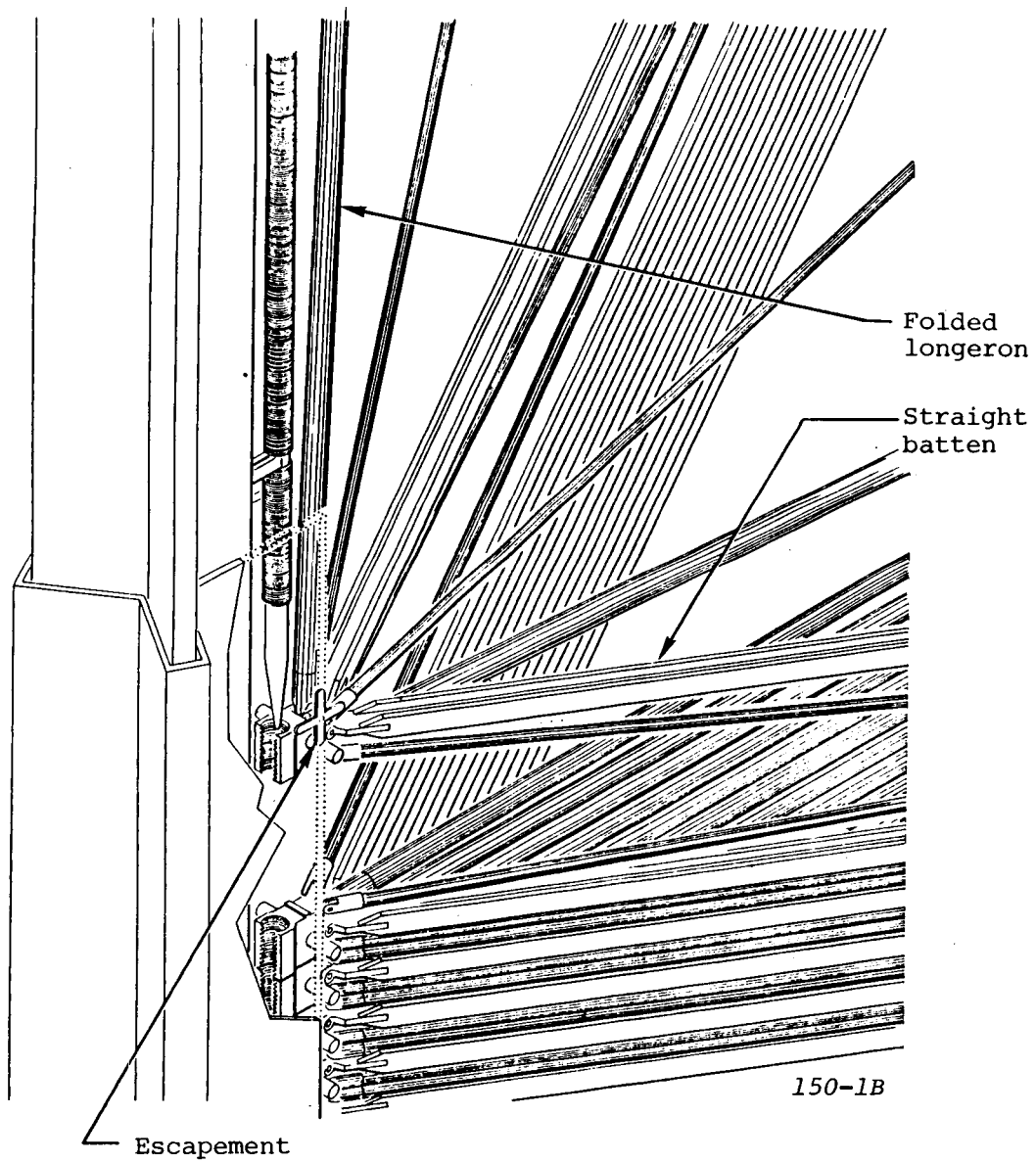

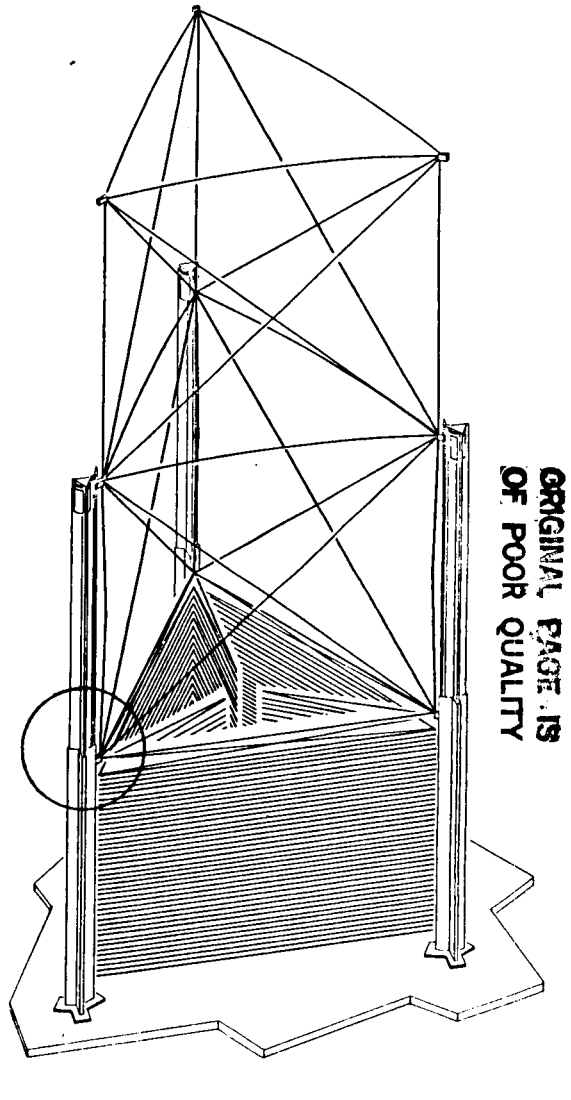

Figure 6. Deployer detail, bay near full extension.

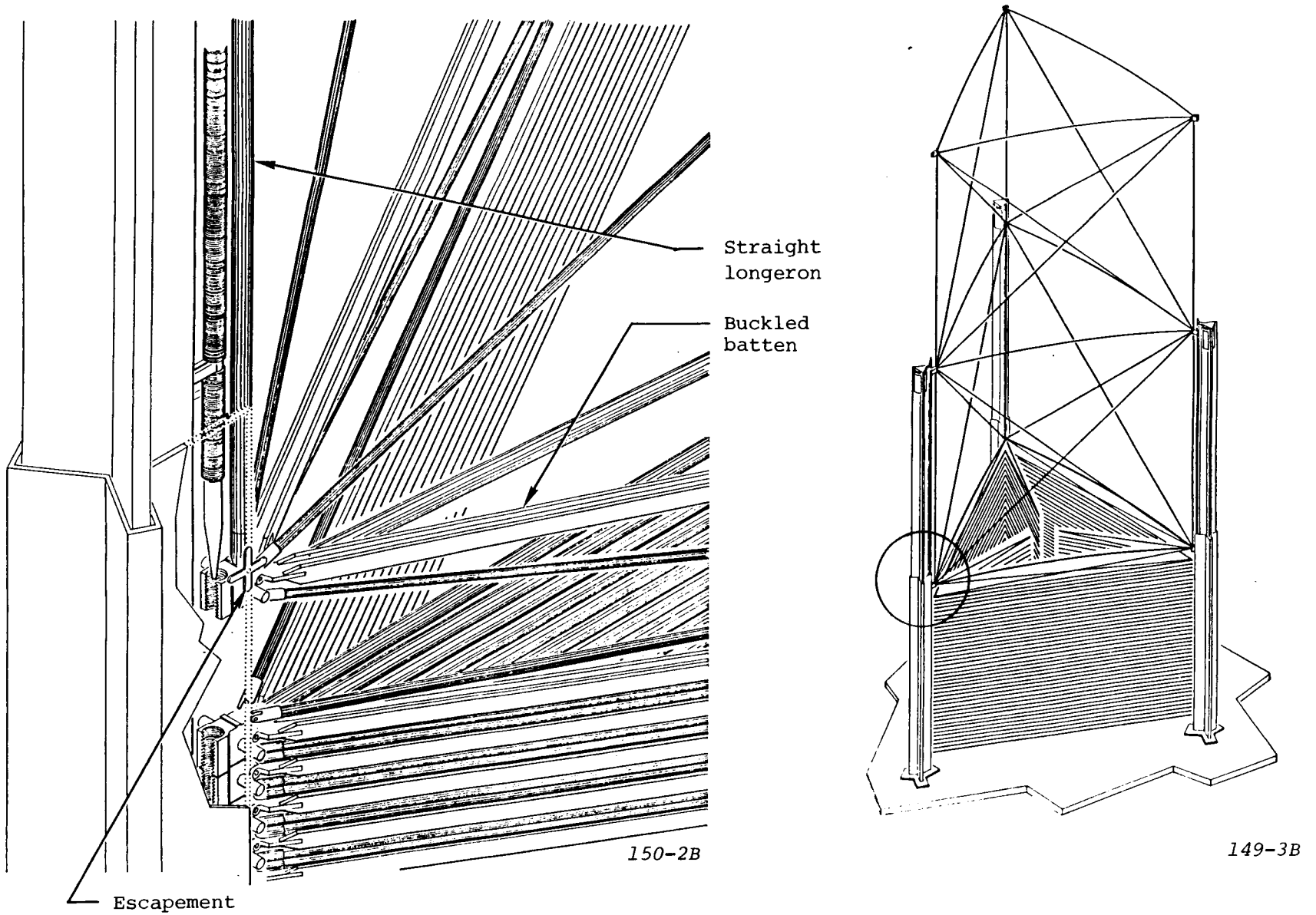

Figure 7. Deployer detail, bay fully extended.

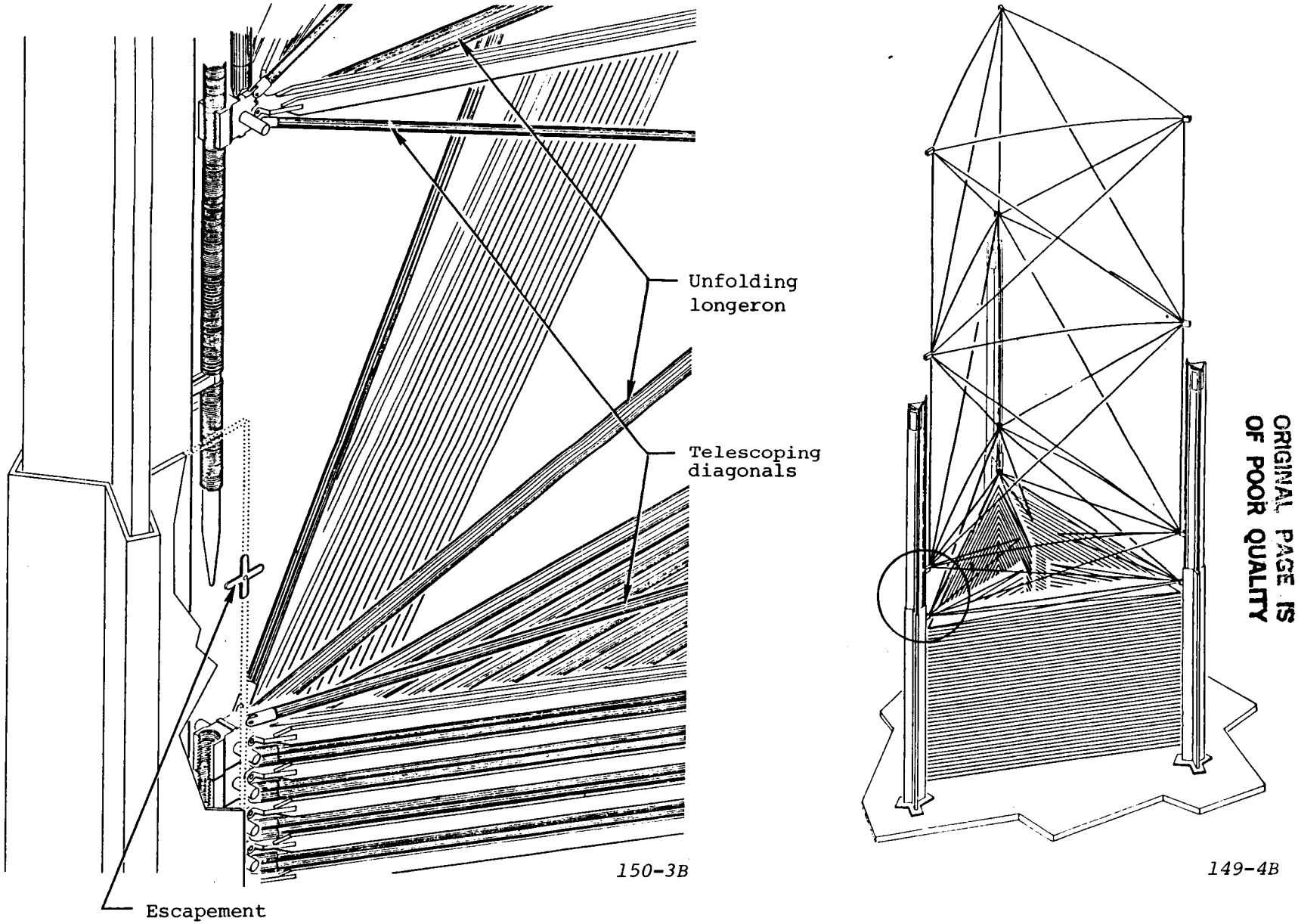

Figure 8. Deployer detail, bay moving up lead screw.

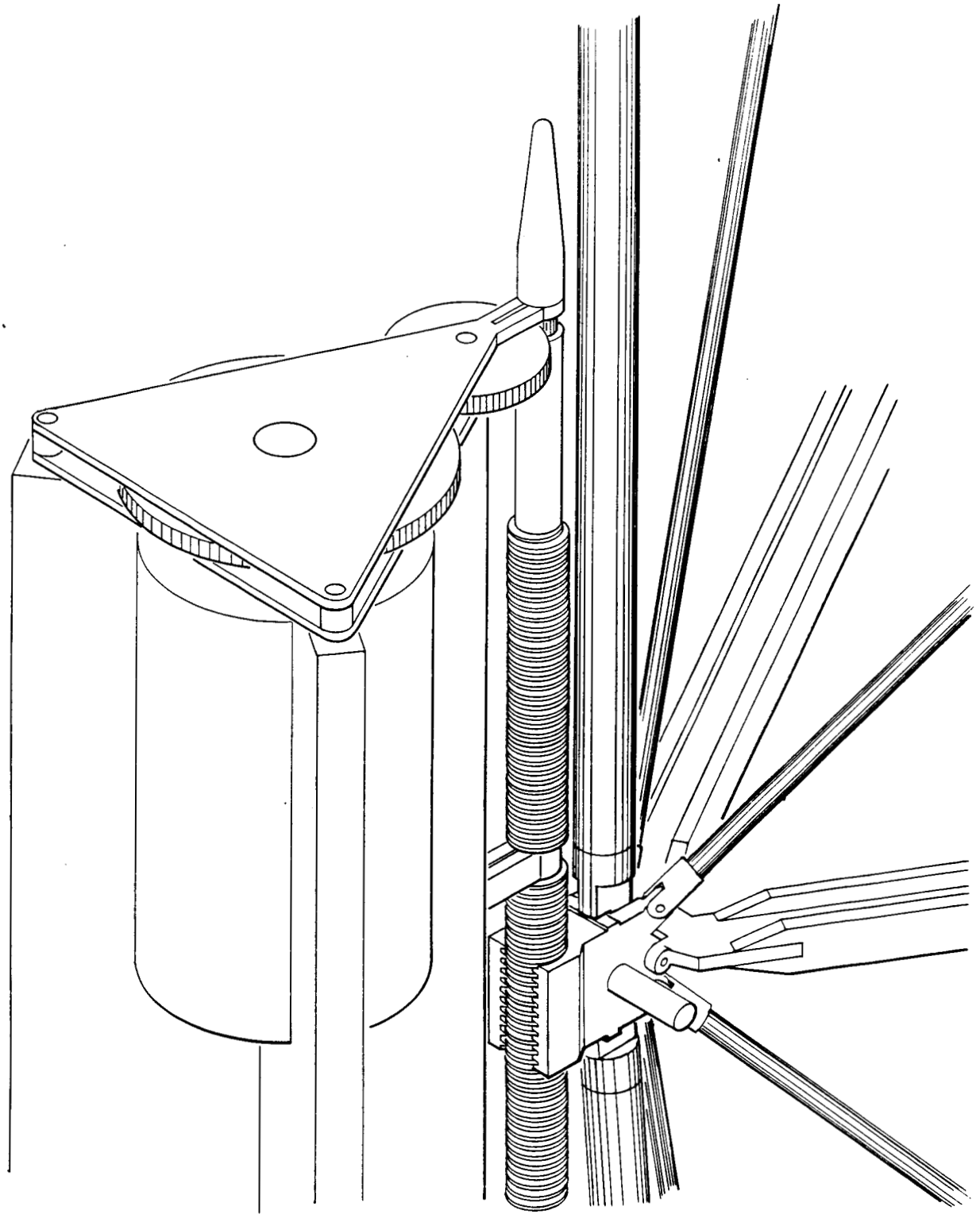

Figure 9. Deployer detail, motor. *153B*

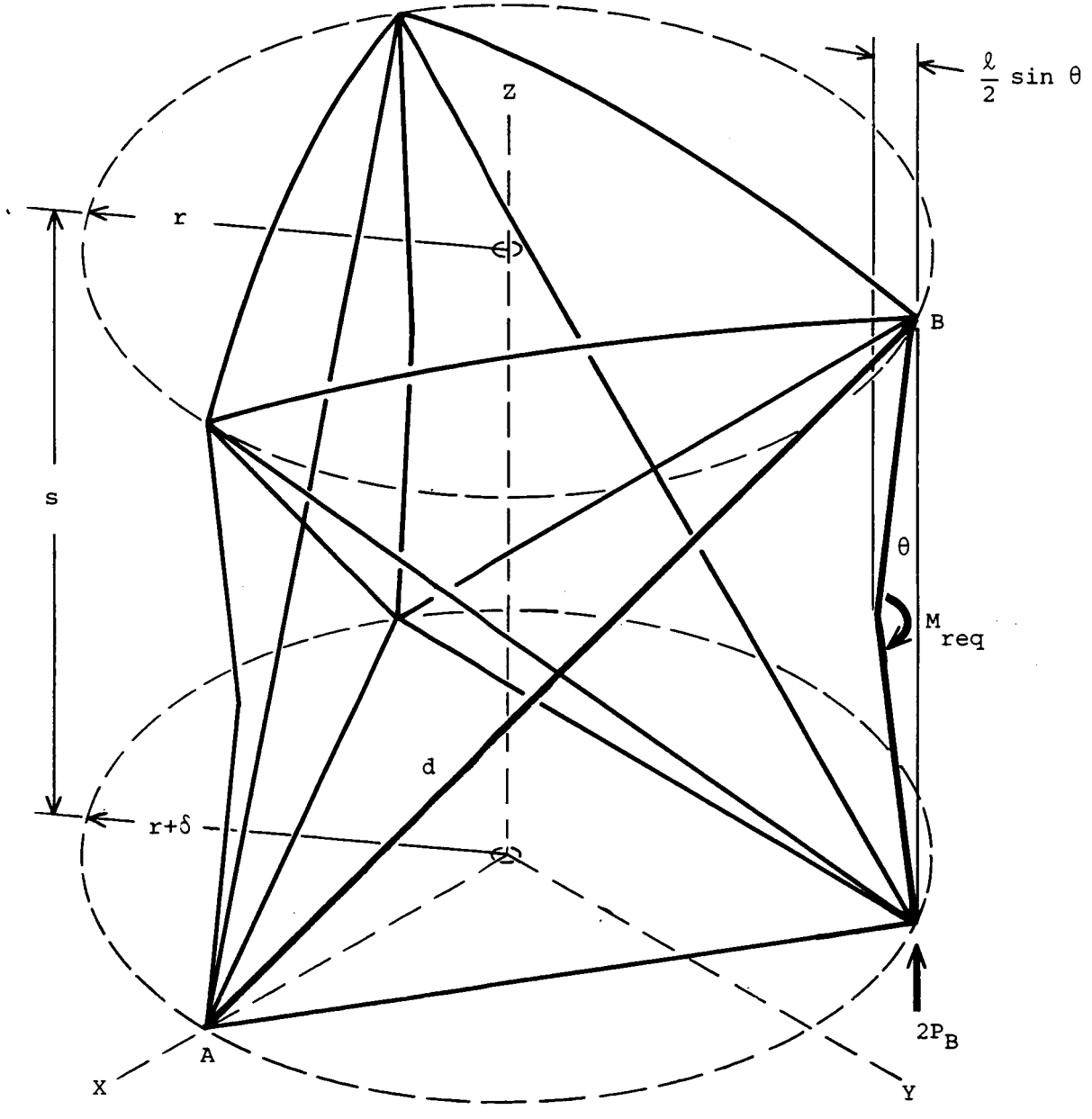

Figure 10. Bay geometry just prior to batten compression. *151A*

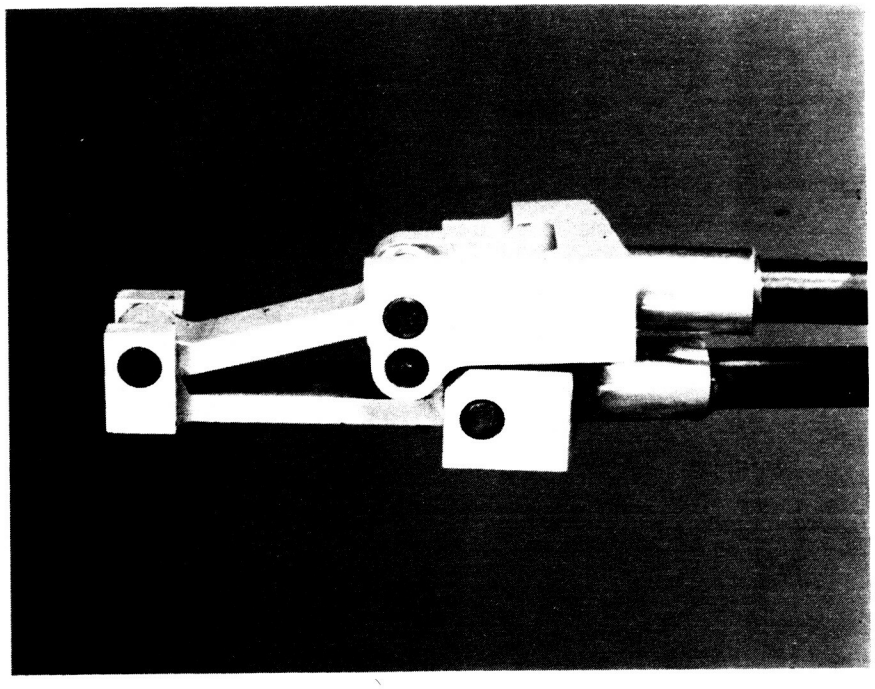

a. Folded P071

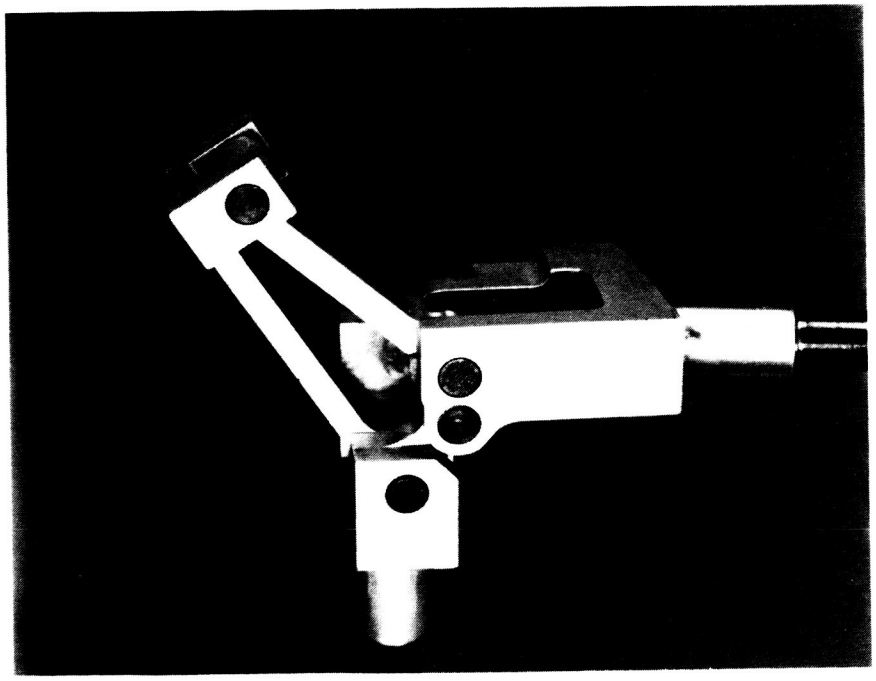

b. Partially opened P072

Figure 11. Almost-over-center hinge.

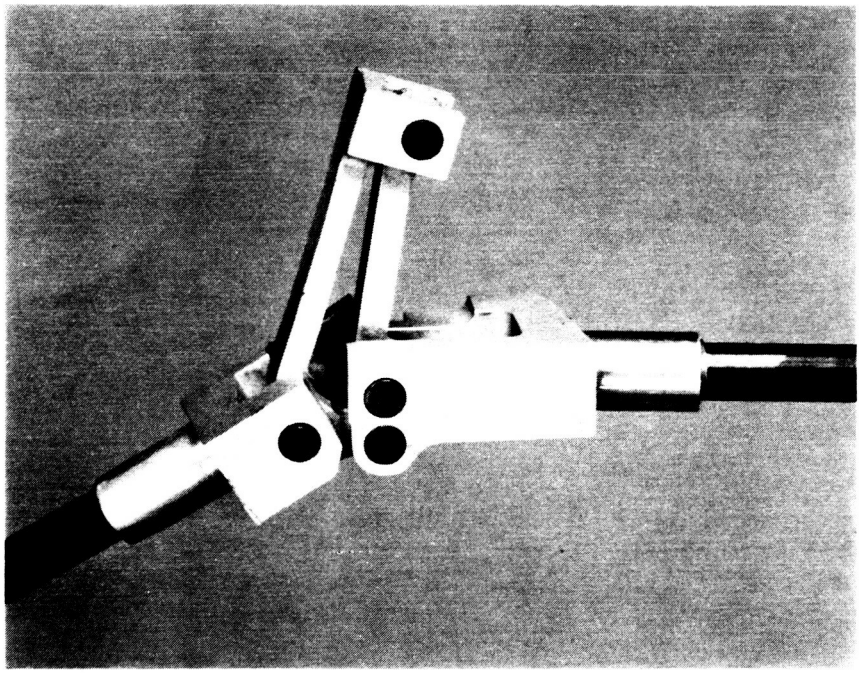

c. Nearly open P073

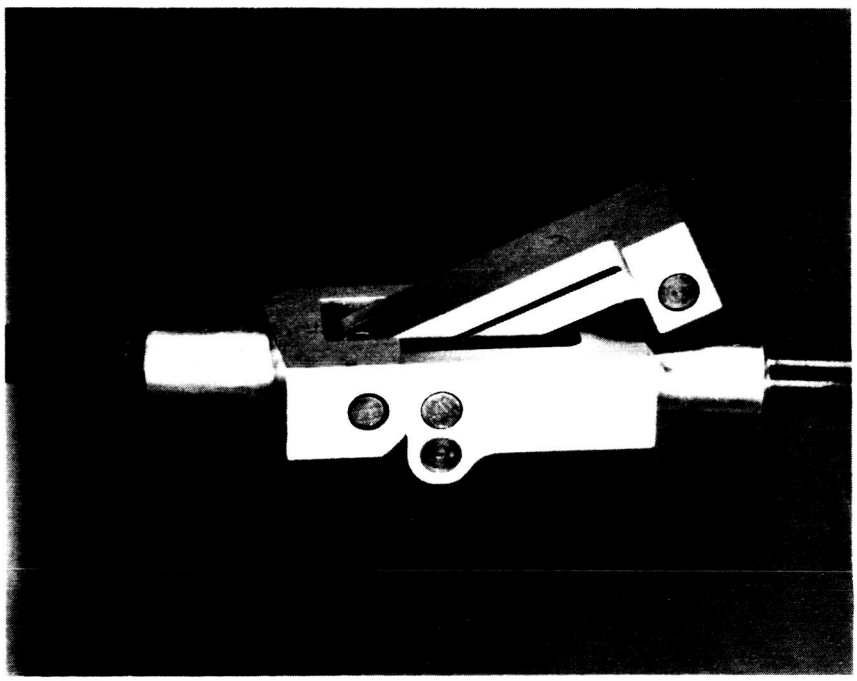

d. Open P074

Figure 11. (concluded).

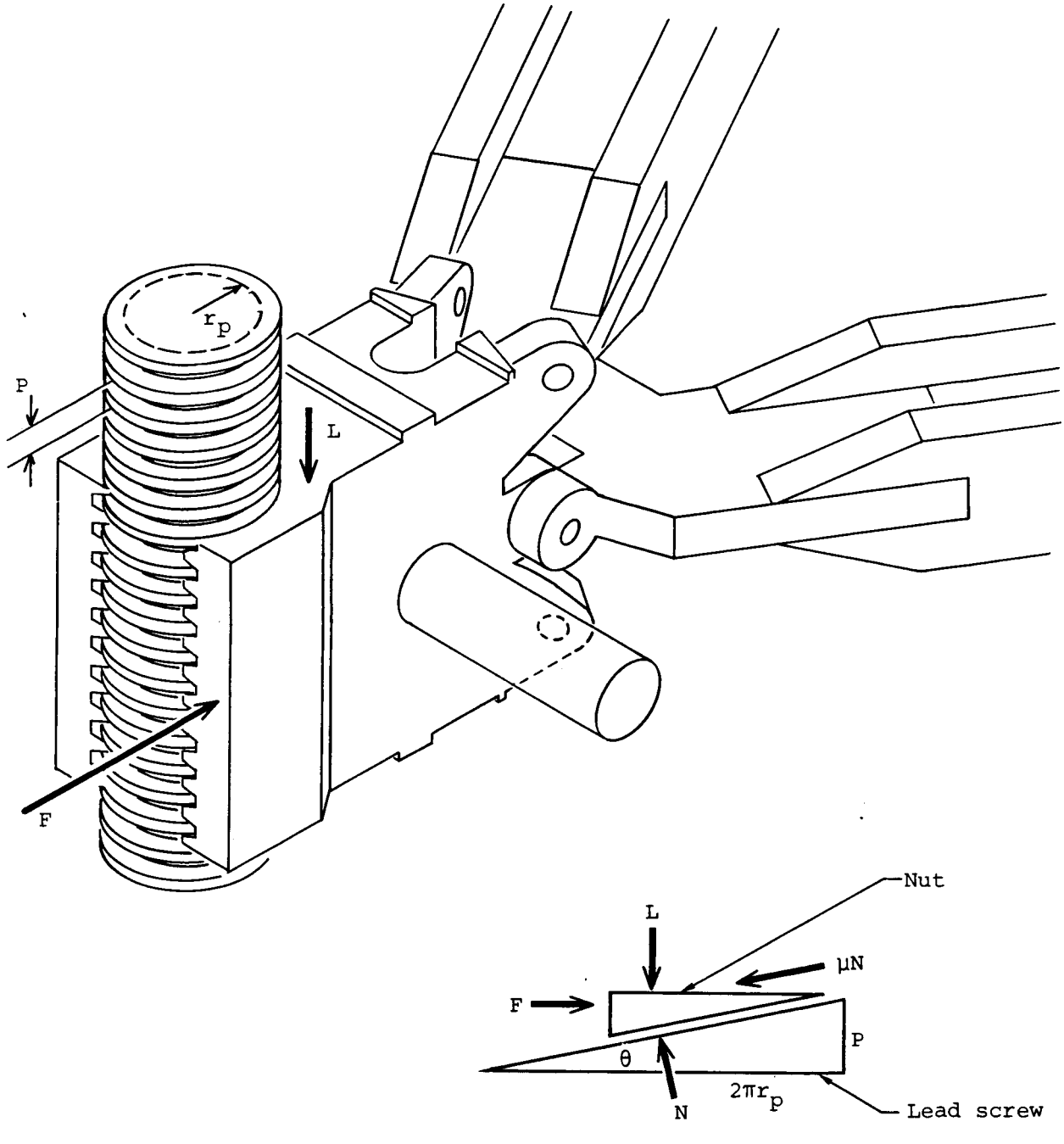

Figure 12. Lead screw torque. *152A*

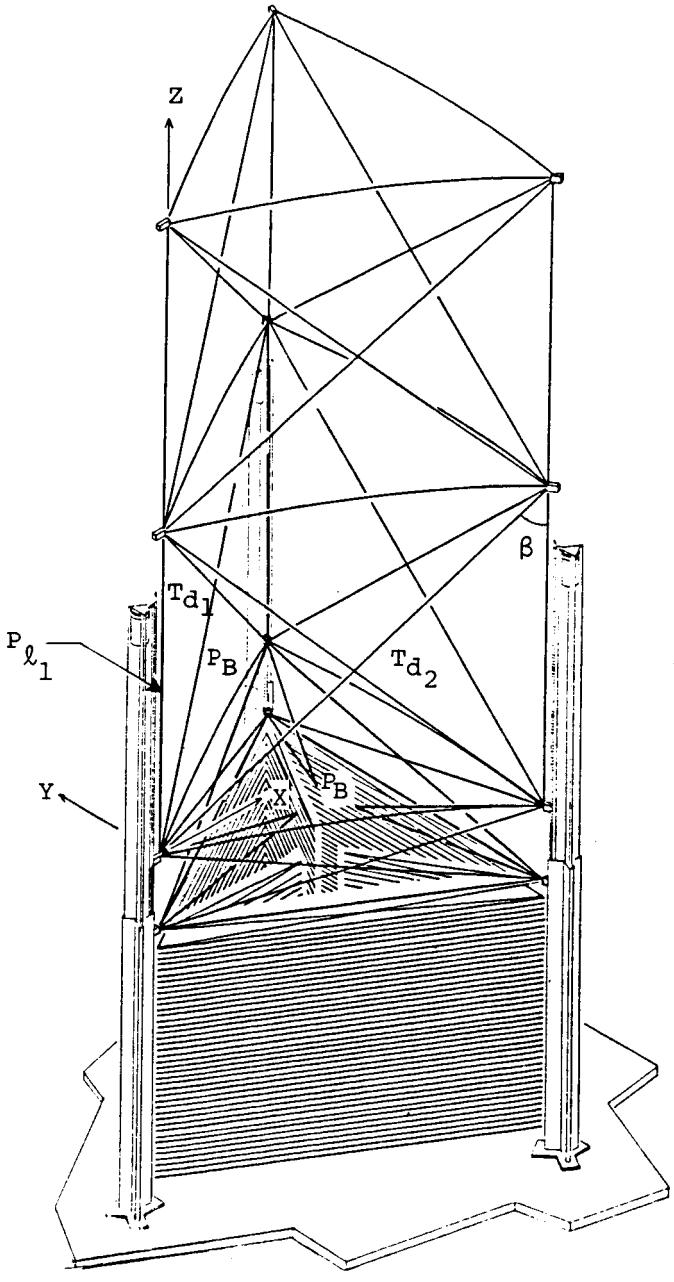

Figure 13. Deployer loads, deploying bay. *149-4-1B*

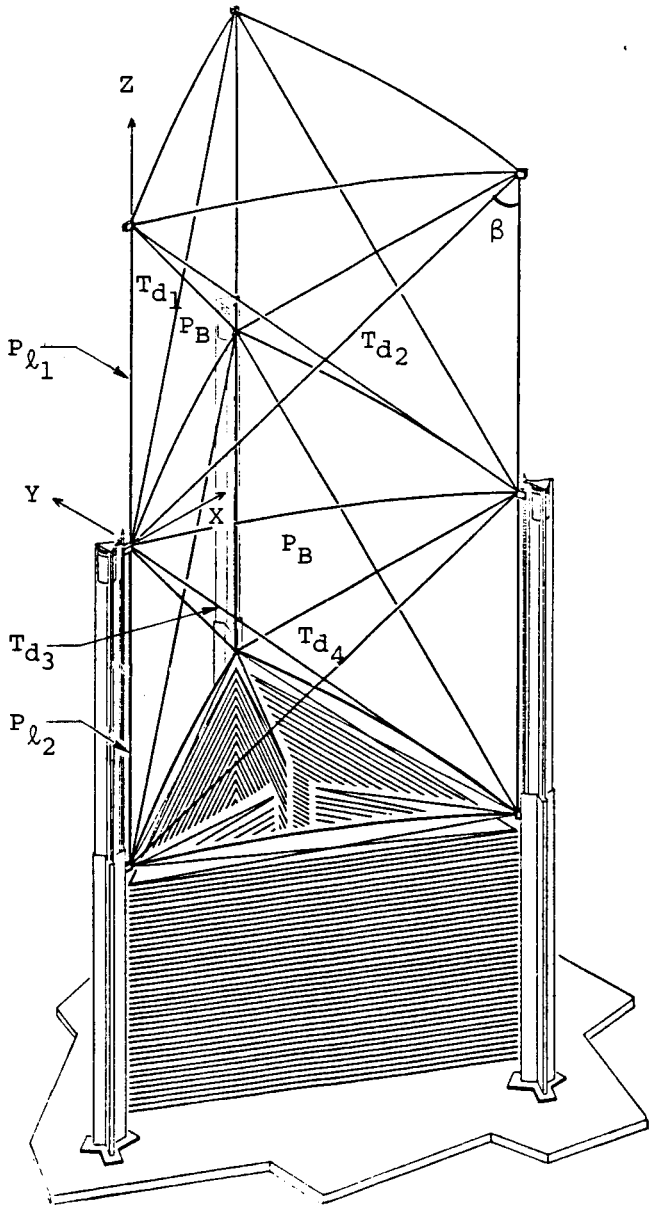

Figure 14. Deployer loads, deployed bay. *149-3-1B*

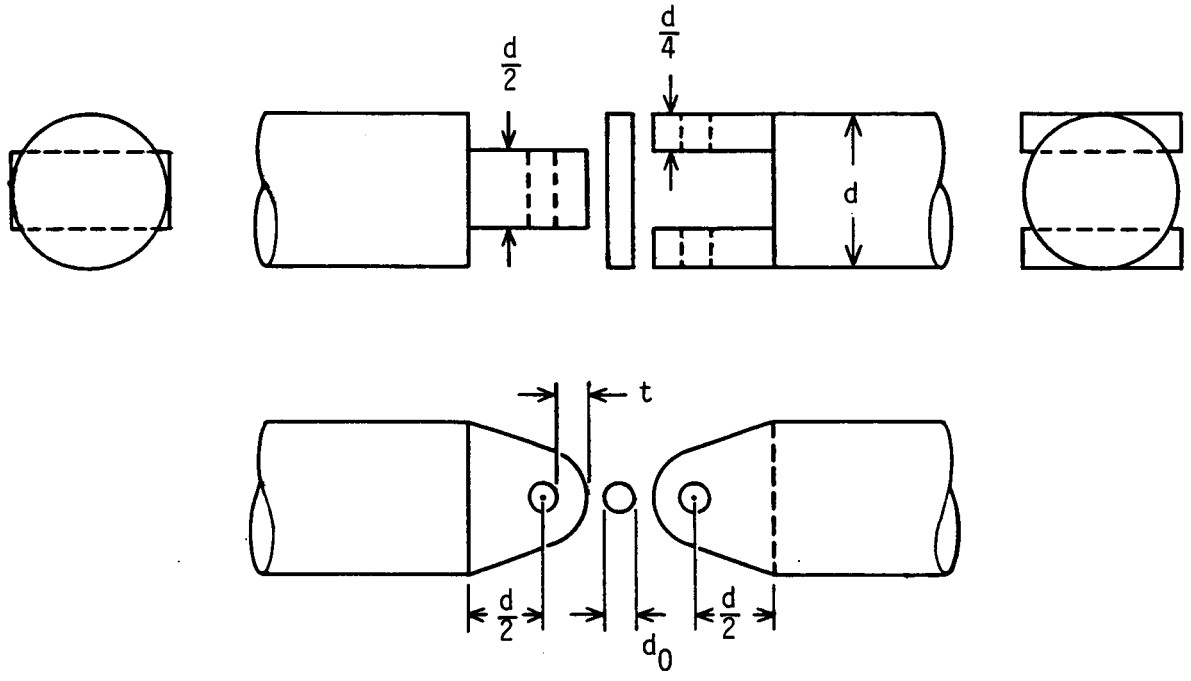

Figure 15. Simple centered-hinge joint. *155A*

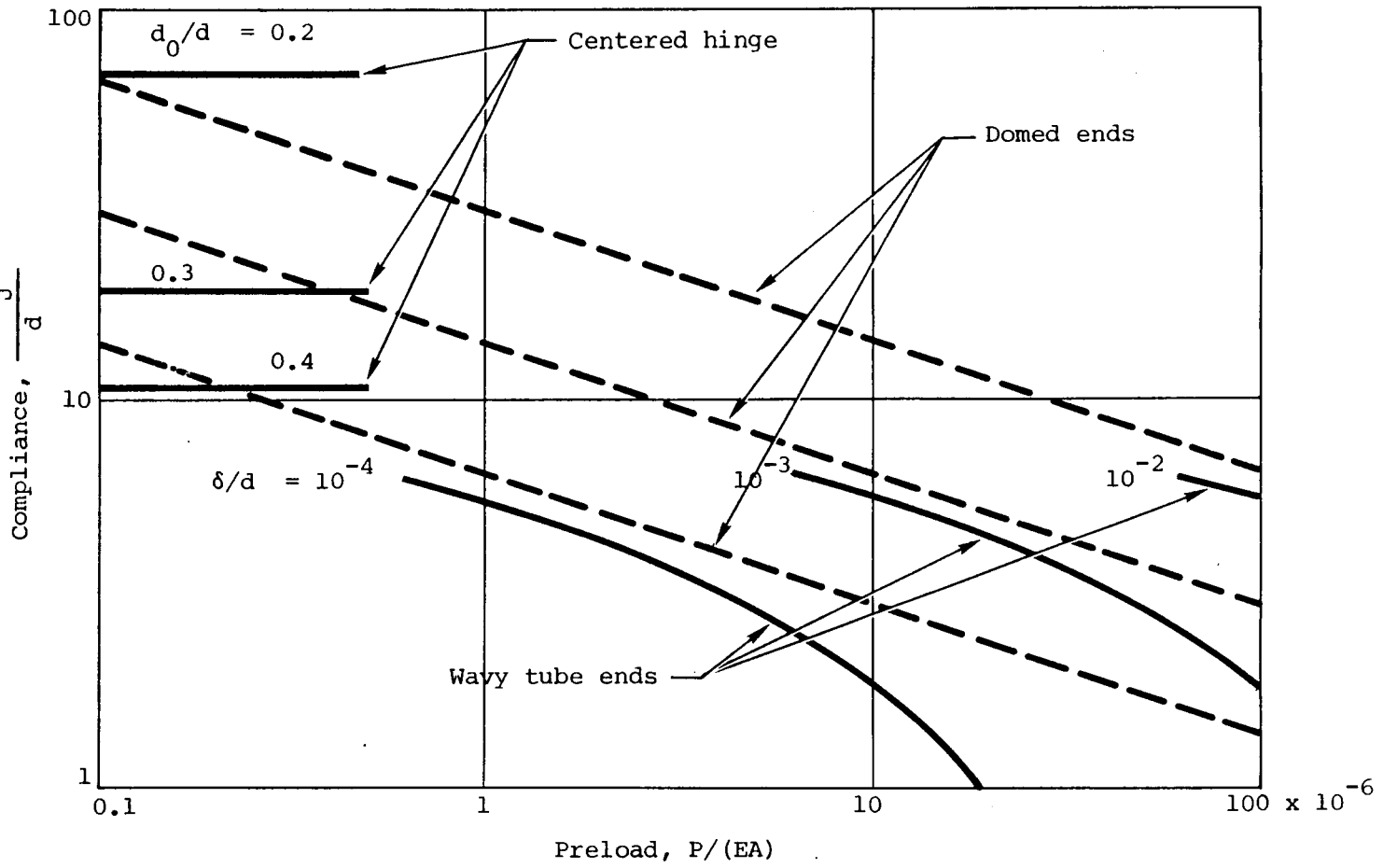

Figure 16. Comparison of joint compliances.

1. Report No.	2. Government Accession No.	3. Recipient's Catalog No.
NASA CR-172461		

4. Title and Subtitle	5. Report Date
Batten Augmented Triangular Beam	February 1986
	6. Performing Organization Code
7. Author(s)	8. Performing Organization Report No.
Louis R. Adams and John M. Hedgepeth	AAC-TN-1130, Rev. A
	10. Work Unit No.
9. Performing Organization Name and Address	
Astro Aerospace Corporation 6384 Via Real Carpinteria, CA 93013-2993	11. Contract or Grant No. NAS1-17536
	13. Type of Report and Period Covered
12. Sponsoring Agency Name and Address	Contractor report
National Aeronautics and Space Administration Langley Research Center Hampton, Virginia 23665	14. Sponsoring Agency Code

15. Supplementary Notes

Langley technical monitor: Marvin D. Rhodes
Final report

16. Abstract

The BAT (Batten-Augmented Triangular) BEAM is characterized by battens which are buckled in the deployed state, thus preloading the truss. The preload distribution is determined, and the effects of various external loading conditions are investigated. The conceptual design of a deployer is described and loads are predicted. The influence of joint imperfections on effective member stiffness is investigated. The beam is assessed structurally.

17. Key Words (Suggested by Author(s))	18. Distribution Statement
BEAM PRELOAD DEPLOYMENT RETRACTION COMPLIANCE	Unclassified-Unlimited CAT. 29

19. Security Classif. (of this report)	20. Security Classif. (of this page)	21. No. of Pages	22. Price
Unclassified	Unclassified	58	